This is to certify that the

thesis entitled

Groundwater Flow and Quality
Behind an Anti-salt Dam in Lower
Casamance Senegal (West Africa)

presented by

Boubacar Barry

has been accepted towards fulfillment
of the requirements for

_____M.S._____ degree in _Agricultural_ Engineering

Major professor

Date___11-11-91_____

PLACE IN RETURN BOX to remove this checkout from your record.
TO AVOID FINES return on or before date due.

DATE DUE	DATE DUE	DATE DUE
———	———	———
———	———	———
———	———	———
———	———	———
———	———	———
———	———	———
———	———	———

MSU Is An Affirmative Action/Equal Opportunity Institution

c:\circ\datedue.pm3-p.

Groundwater Flow and Quality

Behind an Anti-salt Dam in Lower

Casamance Senegal (West Africa)

By

Boubacar Barry

A THESIS

Submitted to

Michigan State University

in partial fulfillment of the requirements

for the degree of

MASTER OF SCIENCE

in

Agricultural Engineering

Department of Agricultural Engineering

1991

ABSTRACT

GROUNDWATER FLOW AND QUALITY

BEHIND AN ANTI-SALT DAM IN LOWER

CASAMANCE SENEGAL (WEST AFRICA)

By

Boubacar Barry

For many years, the Casamance was a food self-sufficient region. Recently, this region has experienced foods deficits because of the persistent drought. Given the shortage of rainfall over the last several years and the increasing accumulation of salt, the number of abandoned mangrove paddy fields is multiplying throughout the region. Along the tidal portion of the river basins one can observe a tendency towards increased salinity of the river bed and increased salinity of the underlying water table. Because of the shortage of available fresh water for leaching the salt out of these fields, site development (polders, anti-salt dams, drainage) has become the only solution to the salt intrusion problem since the early 1970's. Today, more than 20 anti-salt dams have been built in the Casamance region, and rice production has substantially increased. The present study focusses on groundwater flow and quality in a typical valley of the Lower Casamance region. A groundwater simulation model, using the finite element approach for evaluating water movement in the aquifer, is developed. Recommendations for improved management strategies for irrigation behind anti-salt dams are also formulated.

Approved   _Vincent Bruff_____   10-1-91

             Major Professor   Date

Approved   _Robert Bunch_____   11/13/91

             Department Chairperson   Date

A la Memoire de mon Pere

Seigneur, Fasse que les portes du Paradis
lui Soient Ouvertes

AMEN

Ton Fils

ACKNOWLEDGMENTS

I would like to give special thanks to Dr. V.F. Bralts, who served as my advisor. I greatly appreciated his support, and patience in helping me in my research. I would also like to thank the members of my Committee. Special thanks go to Dr. J. L. Posner for guiding my research at home in Senegal, to Dr. J. Bingen for giving the opportunity to study at this wonderful university.

In addition I want to thank my family, Maguette, Tafsir, and Iba my lovely wife and beautiful kids, and my new found Michigan friends, Aliou, Rabi, Jon, Martin, Jim and Mark Pires, who helped me in more ways than they will ever known. Last but not least, special thanks to my mom who gave never ending support and encouragement through my frantic hours.

TABLE OF CONTENTS

viii

LIST OF TABLES

LIST OF FIGURES

LIST OF ABREVIATIONS

CIID   :   Commission International des Irrigations et
Drainages. (International Commission on Irrigation
and Drainage).

CILSS   :   Comite Interetats de Lutte contre la Secheresse
dans le Sahel. (Interstate Commitee for Drought
Control in Sahel).

CNRS   :   Centre National de Recherches Scientifiques.
(National Center for Scientific Research).

FAO   :   Food and Agriculture Organization.

IRAT   :   Institut de Recherches en Agronomie Tropical.
(Research Institute for Tropical Agronomy).

ISRA   :   Institut Senegalais de Recherches Agricoles.
(Senegal Agricultural Research Institute).

NBA   :   Niger Authority Basin.

NGO   :   Non-Government Organization.

OMVG   :   Organisation pour la Mise en Valeur du Fleuve Gambie.
(Operation for the Development of the Gambia River).

OMVS   :   Organisation pour la mise en Valeur du Fleuve
Senegal.
(Operation for the Development of the Senegal River).

ORSTOM   :   Office de Recherche Scientifique et Technique
d'outre Mer. (Office of Overseas Scientific and
Technical Research).

SAED   :   Societe d'Amenagement et d'Exploitation des Terres du
Delta. (Delta Canal Development Corporation).

SODAGRIZ   :   Societe de Development Rizicole. (Rice
Development Company).

SODEFITEX   :   Societe de Development de Fibres Textiles.
(Textiles Development Company).

SOMIVAC   :   Societe de Mise en Valeur Agricole de la
Casamance. (Casamance Agiculture Development Co.)

USAID   :   United States Agency for International Development.

I. INTRODUCTION

A. BACKGROUND.

The West African country of Senegal (Fig.1) is primarily
an agricultural country. In 1980, agriculture accounted for
28 percent of the GNP and provided employment for 80 percent
of the economically active population. The most important
agricultural product in Senegal is peanuts, the mainstay of
the economy.

In recent years, cereal production in Senegal has not
been sufficient to meet consumption needs. Currently, there
is a deficit of about 200,000 tons of cereal grains each year.
For decades Senegal has exported groundnut and imported rice
to cover its food deficit. During the late sixties and early
seventies, due to the rapid growth of urban areas, the failure
of food production, the disruption of peanut production, the
instability of world prices, and the Sahelian drought, the
country has become painfully aware of its dependence on
imported food, namely rice. Since 1977, due to a generalized
drought, Senegal has imported more than 600,000 tons of
cereal. At the present time, domestic rice production covers
only 15 to 30 percent of the country's needs every year.

Because of economic instability arising from the combined

1

Figure 1. Major regions of Africa.

factors of heavy dependence on imported food and unstable
rainfall patterns, irrigation and full water control systems
along the major rivers have become a main priority for the
Government of Senegal.

Although most of the irrigation systems have been built
in the Senegal River Valley (Fig.2), an ambitious program of
soil and water management has developed during the early
1980's in the Lower Casamance region to improve food
production.

Site developments in Lower Casamance have considerably
increased during the last decade primarily because of the
drought situation. Today, more than 20 dams have been built
in the region in order to protect the paddy fields against
sea water intrusion during the high tides of the dry season,
and to store fresh water during the rainy season. It is
estimated that more than one third of the paddy fields were
abandoned in this region because of the high salinity of the
soil and water table. The fresh water retained behind the
dams helps to leach the salt out of the paddy fields and
facilitates rice growth after reclamation of the abandoned
paddy fields.

The rainfall shortage and the problem of salinization
have affected not only the polders but also the most
productive paddy fields located on the first level terraces.

In most of the valleys where small anti-salt dams have been built, rice production has substantially increased. Perhaps the best example of this increase is the Katoure Valley where, for more than one decade, the paddy fields affected by the salt were abandoned. Only two years after the construction of the dam, the average rice paddy yield in those same fields was 3.5 tons per hectare. However, many problems still remain to be solved. In many paddy fields located essentially in the lower lands, the water table rises fast at the beginning of the rainy season when its salinity is already very high. In some cases, the water table salinity reaches levels twice that of sea water, which is 35 g/l. Most of the salt is not taken out of the system. Rather, it is diluted as the reservoir fills up with fresh water. With the reduced amount of precipitation each year, the water table salinity tends to rise fast reaching a concentration that can be detrimental to the paddy plant's growth. This situation can lead to a big loss in grains production, mainly when there is no more fresh water stored in the reservoir and evapotranspiration is high.

Since 1984 many studies have been conducted by the research teams of ISRA and ORSTOM in site developments where anti-salt dams were already built.

The following analysis of groundwater management will focus on the Katoure valley where the first anti-salt dam was
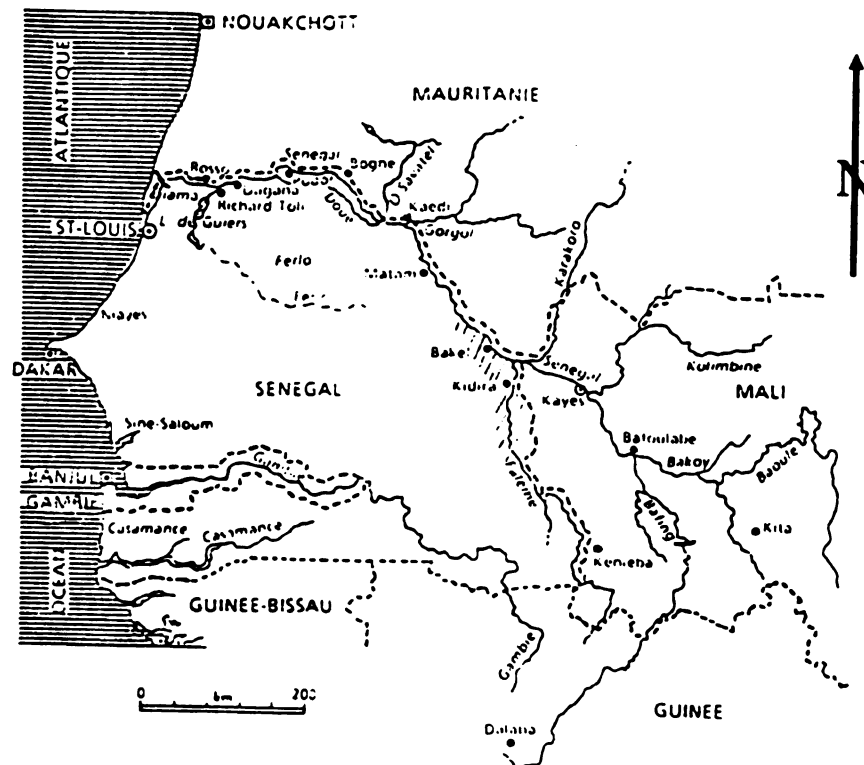
Figure 2. Map of Senegal's rivers.

built in 1984.

The Katoure site is representative of the Lower Casamance region from a soil and hydrologic point of view. The social impact and economical aspects of the dam have also been studied recently, and both show a need for defining strategies for water management, especially during years with rainfall shortage.

B. SCOPE AND OBJECTIVES.

The overall goal of this study is to increase crop production and economic returns to farmers in the Lower Casamance region of Senegal. This goal will be achieved through an improved understanding and management of anti-salt dams.

The specific objectives of this thesis are to :

1. study the groundwater flow and quality in a typical valley of the Lower Casamance region.

2. develop a groundwater simulation model for evaluating water movement in the aquifer.

3. evaluate improved management strategies for irrigation behind anti-salt dams.

II. REVIEW OF LITERATURE AND THEORY

A. IRRIGATION AND DRAINAGE

The following section consists of a review of irrigation methods used around the world and those specifically employed in the Sahel region of Africa.

1. World.

Worldwide irrigation has expanded dramatically in this century. In 1900 there was about 40 million hectares, and today we find approximately 270 million hectares of irrigation on 18 percent of the cultivated land. Irrigation provides approximately one third of the world's food.

The international rate of irrigation development in the 1960s averaged almost 6 million hectares a year (FAO 1986). The most rapid growth has occurred in India where, in the 1960s, the gross area expanded from about 28 million to 37 million hectares, and today it is about 55 million hectares. In the 1980s, the worldwide rate of growth has declined slightly because of economic recession, adverse terms of trade for agriculture, and new emphasis on rehabilitation and modernization of existing systems. Reliable figures are not available, but the current rate of growth has probably fallen

to about 4 million hectares a year. Table 1 shows growth in irrigation development by continents since the middle of the century.

In general the objectives of irrigation development have been either to achieve self sufficiency in food and fiber or to maximize economic efficiency in the use of land and water. The former objective is essentially the developing country's and the latter the developed country's. It is interesting to reflect on some of the factors that have influenced the pattern of growth in irrigation and drainage over the fifty years.

From the middle of this century new technologies that had remained latent during World War II were applied to agriculture throughout the world. At the same time, large investments were made in irrigation, particularly in countries such as India, Sudan, Egypt, and Pakistan where there has been an established tradition in irrigated crop production. As a result, grain production rose about 3 percent a year in the period from 1950 to 1973 (FAO, 1986). Of the new technologies, the most dramatic in its effect was the introduction of new crop varieties in the late 1960s, the so-called "Green Revolution."

A second event which affected agricultural production and the value of irrigation and drainage was the oil crisis of

1973 with its second wave in 1979. The rise in oil prices contributed to a rapid decline in the growth rate of grain production from about 3 percent to 2 percent in the period from 1973 to 1977, and in recent years it has fallen toward 1 percent. Regions with poor climates and soils are the most affected as we see from the present situation in Africa. The underlying reason is that high oil prices mean high input costs, so areas with marginal yields fall out of production.

Table 1. Gross irrigated areas by continent
(million hectares). (Source: FAO 1986)

Regions	1950	1960	1970	1986
Europe (incl. part USSR)	8	12	20	29
Asia (incl. part USSR)	66	100	132	164
Africa	4	5	9	13
North America	12	17	29	34
South America	3	5	6	9
Australia and Pacific	1	1	2	2
Total	94	140	198	271

In many countries where irrigated land represents a high proportion of the total cultivated land, the available water resources are approaching the economic if not the physical limits of exploitation. This applies to India, Sri Lanka, the southwestern United States, Egypt and Sudan. There are small island countries like Mauritius and arid zone countries like Somalia and Botswana that need irrigation but have a very poor

distribution of water resources in relation to irrigable land.
Possible options in regions of water shortage are to :

(a) construct more storage reservoirs,

(b) undertake major interbasin transfers of water,

(c) better integrate use of ground and surface
waters,

(d) economize on present water use by raising water
management standards of irrigation efficiencies.

In some countries, the correct solution is to undertake
most, if not all, of these measures as part of a long term
investment program, taking into account that some of them are
longer term than others. This is indeed the policy being
followed by countries such as India and Mauritius.

The improvement of irrigation efficiency is the most
vital requirement of our time. A survey by CIID has shown
that in surface irrigation systems, application efficiencies
vary from 35 to 75 percent and conveyance efficiencies from 30
to 90 percent. The overall efficiencies fall mostly between
10 to 50 percent. Many large surface systems in Asia have
efficiencies in approximately the middle of these ranges or
about 30 percent compared with about 37 percent efficiency in
some developed countries. By contrast, countries with more
advanced drip systems have overall efficiencies of about 60
percent. However, such advanced systems are mainly applicable
to industrialized countries or where crops of high value are
grown.

1.1. Advanced Technology.

New irrigation technology plays an important part in the achievement of better irrigation efficiency. In countries with advanced technologies, water use per hectare is about half that of the less advanced technologies.

Rapid increases in energy costs and the continual competition for limited water resources have been the impetus for continuing research to develop new irrigation systems and improve technology. Advanced technology includes the use of surface irrigation sprinklers, microsprinklers, and drip irrigation. Recently, more attention has been given to subsurface systems and to subsurface drip systems that inject water into the root zones with great efficiency.

1.1.1 Sprinkler Irrigation.

The development of electronics in the 1960s and microprocessors in the 1970s advanced this irrigation method to one of the most efficient and reliable irrigation methods available today. Further improvements using the concepts of low-pressure drop tube and micro-basins developed by Lyle and Bordovsky (1983) are under way. For example, with these improvements, they reported irrigation efficiencies of greater than 95 percent with a linear model system. Heerman et al. (1984) adapted computer control and optimization technology to center-pivot systems. Similar advances have been made in water distribution, measurement, and technology

for system control. In developing countries, most irrigation projects still performed well below their potentials (Plusquellec, 1985). Improvements can be made without highly sophisticated technology. For example, Plusquellec emphasizes that not all automation of water control needs to be computerized.

1.1.2. Surface Irrigation.

Surface irrigation has been used for centuries. Major technological advances in other fields have been used to improve technology for surface irrigation. For example, the adaptation of laser controls to land leveling equipment in the mid 1970s had a major impact on technology for leveling basins. With laser-control equipment, 4 to 8 hectare basins can be leveled so that 85 percent of the soil surface is within 15 mm of the mean elevation. Irrigation efficiencies of 70 to 100 percent are now being achieved with level basins (Dedrick et al., 1982).

Surge flow, or cycling the flow to irrigation furrows, is a technique developed in the late 1970s to increase the advance of water in furrows with a given amount of water. This has made it possible to reduce runoff and improve irrigation uniformity on many soils.

The commercial development of automatic equipment using low cost valves and electronic controllers has played a major role in the development of this technology. Another new

method of controlling water delivery to furrows is a method called "cablegation" (Kemper et al., 1981). It has enabled the automatic and uniform distribution of flow to individual furrows.

1.1.3. Trickle Irrigation.

Trickle irrigation technology, often called drip irrigation or microirrigation, has advanced greatly during the past two decades (Bucks et al., 1982). These systems, when properly designed, installed, and operated, can provide excellent control of irrigation water (Bralts et al., 1987). Plugging of emitters has been a major problem, but filtration and chemical treatment of water minimize these problems.

Evapotranspiration for most close-growing crops is essentially the same with these systems as with other systems. However, decreases in seasonal evapotranspiration of 10 to 15 percent can be achieved with buried, widely spaced trickle lines because of reduced evaporation.

These modern technologies are rapidly penetrating the developed countries where the cost of water is usually charged by volume. They are unlikely to penetrate the developing world until a more realistic tariff structure is adopted for water.

1.2. Cost.

Irrigation is a high cost form for agricultural

development, and big projects have long lead times from project inception to full development.

Costs vary widely throughout the world depending on the type of system, water source costs, size of project, and available resources for construction. The lowest cost of new major irrigation systems are found in Asia, particularly in India, where the surface systems cost from $2,000 to $4,000 per hectare. In other countries where projects are large enough to provide economy of scale, costs are around $5,000 per hectare.

In regions where projects are small and where there has been no long tradition for irrigation, costs are often $10,000 per hectare and more. The higher range of costs is typical of most of sub-Saharan Africa. There, irrigable land is found in small scattered entities, which results in not only a high average cost of development, but also a higher cost of infrastructure for transportation, marketing, and supplies that must be improved as part of the project costs.

1.3. Drainage.

In drainage development, statistics are very limited. However the majority of growth in drained areas has been in Europe and North America. The pattern has shifted in recent years to other regions, including the Soviet Union, China, Pakistan, Bangladesh, and the Middle East, where the old irrigation systems are suffering from waterlogging. In some

regions of the world such as Bangladesh and Cambodia, poor drainage and flooding represent the main constraints on agricultural production.

The development of corrugated plastic tubing in the 1960s greatly changed subsurface drainage technology. About 90 percent of the drain tubing being installed today is plastic instead of clay tile.

The adaptation of laser control to drain installation in the 1960s also advanced this technology. Advances in drainage technology have greatly reduced the cost of drainage, but design techniques and criteria for subsurface drainage of irrigated land have not changed. Today new techniques are being initiated in humid regions. These techniques include controlling drainage outflow and using the same system for subirrigation.

1.4. Human Resources.

Of the 271 million hectares of irrigated land in the world, 75 percent are in developing countries. Many of these countries suffer from shortages of varying degrees in human resources with trained management capability. Even where there is an adequate supply of technical resources, management resources may be lacking in many sectors. There is an urgent need for training in management technology and irrigation management in particular.

2. Africa.

Africa has not developed irrigation to the same extent as other developing areas, namely Asia. Only a little more than 0.3 percent of the 2,818 million hectares covered by FAO's 51 African member nations is currently irrigated. By contrast, India which has only about one tenth of the surface area of Africa, irrigates nearly five times as much land.

The development of irrigation in Africa has also been very concentrated. The 13 million hectares that are currently irrigated amount to about 5 percent of the land in Africa with permanent and temporary crops. One in every 20 of Africa's cropped hectares is irrigated. However, in Egypt, 98.6 percent of the cropped area is irrigated. About one half of Africa's irrigated area is in Egypt and Sudan. Two other countries, Madagascar and Nigeria, account for a further 20 percent of the irrigated area (FAO, 1986).

The extent to which areas are developed is not uniform throughout the continent. Most of what could be described as "formally organized" irrigation -typically medium- or large-scale projects - occurs in Egypt and Sudan. This kind of irrigation covers about two thirds of the irrigated area. The other one third is traditional, small-scale irrigation in which simpler technologies are used and where there is often only a partial control of the irrigation water. This form of

irrigation is somewhat more widely spread; yet, 81 percent of small scale irrigation occurs in just five countries.

The distribution of the irrigated area over Africa's major regions is shown in Table 2.

Table 2. Distribution of irrigated area over the African region. (Source: FAO 1986. *Refers to the total irrigated area in 51 FAO Member Countries*)

Regions	Irrigated Area (1000 hectares)	% of Total
Mediterranean and arid North Africa	4192	47
Sudano Sahelian Africa	2242	25
Humid and sub-humid west Africa	937	10
Humid Central Africa	18	-
Sub-humid and mountainous East Africa	1147	13
Sub-humid and semi arid Southern Africa	433	5
Total	8969	100

The value of irrigation in Africa is easily demonstrated. Although irrigation occupied only 6.5 percent of 124 million hectares of cultivated land in 43 countries during 1970 - 1980, it provided 20 percent of the value of all the agricultural crops grown in those countries. Irrigation increased the value of agricultural production per hectare by

more than three times.

The need to expand irrigation in Africa arises from the present food and agricultural crisis, which has been developing for several decades. As the FAO study "African agriculture: the next 25 years" (1986) recently reported, there has been a widespread decline in per capita food production in Africa. Because Africa's population is likely to double over the next 25 years, a failure to take steps needed to halt this deterioration "could lead to a situation in which half of Africa's people would be dependant on food imports and food aid from developed countries... and to widespread famine with destabilizing consequences both in and outside Africa".

Such a result is by no means inevitable. African soils can be made productive with good management, and the use of more and improved inputs such as seeds and fertilizer. Other measures include halting soil erosion, improving fertility, and adopting agricultural policies that will provide African farmers with the incentive they need to grow more.

3. Sahel.

The term "Sahel" refers to a climatic zone encompassing the lands immediately south of the Sahara which receive between 100 to 200 and 500 to 600 mm of rainfall per year

(authors differ in their specification of the zonal limits).
In the Sahel zone the risk of inadequate rainfall is so great
that unless farmers have access to at least supplemental
irrigation they will experience frequent crop failures.

Politically , the Sahel region consists of a chain of
former French African nations stretching in a band across the
southern margins of the Sahara from Senegal to Sudan.   In
sequence from west to east there is Cape Verde (islands
offshore Senegal to the west), Senegal, Gambia, Mauritania,
Mali, Burkina Faso, Niger, the northern portion of Nigeria,
Chad, and even part of Sudan (Fig.1).

The heavy rainfall received in the highlands of Guinea
drains north towards the Sahara rather than south towards
the ocean.   Thus, the Niger and Senegal Rivers traverse
hundreds of kilometers of semi-arid land carrying water
derived from far-distant highland sources.

The fossil (600 and 40,000 years ago) and subsurface
drainages are the remnants of wetter periods that the Sahel
enjoyed.   While no longer carrying surface flow, these
drainages may yet contain substantial subsurface storage
suitable for tubewell extraction.

In Sahelian Africa, water control has played a relatively
minor part in agricultural development. This has been limited
historically to traditional small scale irrigation in drought-

prone areas and the reclamation of small swamplands. However, in recent decades there has been a move toward the development of larger schemes, usually for the commercial production of crops such as sugarcane, cotton and rice.

Irrigated farming is as yet poorly developed in the Sahel. In 1976 there was full or nearly total water control for only 80,000 hectares, less than 1% of the total cultivated lands. An additional 150,000 hectares were irrigated with partial water control.

Irrigation was first introduced by the French Colonial Administration quite some years ago with the first large scale total water control development dating back to the 1930s in the Office du Niger. The aim then was to develop cash crops especially cotton, using modern agricultural techniques.

These projects were later added to with less expensive, partial water control elements to be used to produce food grains for local consumption.

After independence, the Sahelian Governments wanted to further develop irrigated farming, with emphasis on rice production, but have not been able to rapidly undertake new installations.

There are undoubtedly several explanations for the current slow rate of irrigation development:

(a) up to now the Sahel has obtained its food through

extensive, traditional, dryland farming without costly investments. This has been supplemented by flood recession crops grown along the major rivers. Irrigated farming was not considered essential for food production.

(b) a certain number of irrigation projects were not resounding successes and all profits accruing to the community were far too small to cover any new installation investment costs. In some cases, not even the operating and maintenance costs could be recuperated and some installations have deteriorated.

(c) projected crop yields per hectare are in general considerably smaller than the planners predicted.

(d) lack of trained personnel mainly for management staff, and high cost of intra-Sahelian transport of materials and goods.

Notwithstanding these handicaps, irrigated crops have already contributed substantially to feeding the Sahel. In 1975-1976, nearly 40% of the rice consumed in the Sahel was produced using modern irrigation, 20% from rain-fed or flood recession cultivation and only slightly over 40% was imported (Club du Sahel, 1979).

The Sahelian countries already rely heavily on irrigation for their rice supply, and since consumption is increasing,

they will either have to develop irrigated agriculture or become increasingly dependent on foreign imports.

The last drought demonstrated the importance of hydro-agricultural installations with total water control as a guarantee for food production. Installations with partial water control proved to be far more vulnerable to the effects of drought, since shallow river waters only suffice to irrigate a small part of the prepared lands. This has encouraged the Sahelian Governments to emphasize the development of irrigated agriculture and accelerate plans for the development of major river basins.

Table 3 gives the estimate areas to be irrigated in several Sahelian countries.

The irrigation systems encountered in the Sahel Region are very diverse. The most frequent found systems are the Traditional, Natural Flooding, Recessional, Controlled Flooding, Total Control, and Basin Control systems. The following is a description of these methods.

3.1 Traditional Labour Intensive Systems

Three important traditional systems that are found in the Sahel are Calabash irrigation, Shaduf irrigation, and Dallou irrigation.

Table 3. Area to be irrigated in the Sahelian Region by Kindell Consult. (1,000 hectares).

Countries	1976	1982	1990	2000
Gambia	1.5	9.5	14	19.7
Burkina Faso	7.7	21.3	58.8	104
Mali	107	125*	160*	132*
Mauritania	1.4	15	30	70
Niger	4.8	17.5	33	52.5
Senegal	96	33.3*	83.5*	160*
Chad	5.8	23.8	49.3	71.8

* *These figures comprise new land developments and rehabilitation of existing perimeters.*

irrigation.

(a) Calabash irrigation: a hand delivery of water onto a field. It is found in scattered isolated areas throughout the Sahel with usually vegetables being the dominant crop grown.

(b) Shaduf irrigation: a traditional water lifting device that has probably diffused into the area from the Nile Valley. The shaduf comprises a log-suspended rod with a bucket at one end and a weight at the other allowing water to be lifted and swung around for depositing into irrigation channels.

(c) Dallou irrigation: not a widely practiced system. Water is lifted by oxen from wells that are 4 to 5 meters deep, and distributed throughout the plot by channels.

3.2. Natural Flood Irrigation.

Two types of natural flood irrigation occur in the Sahel.

(a) Flood Plain Irrigation: in flood plain areas of rivers and streams where annual flooding occurs, rice is quite often planted. Rice is usually sown at the beginning of the rainy season and allowed to germinate before the arrival of the floodwater. This system is risky and the rate of success is not high.

(b) Depressional Irrigation (Bas-fonds): another type of natural flood irrigation is often carried out in depressions where the water table rises during the rainy season to inundate the depression.

3.3. Recessional Irrigation (Culture de Decrue).

In areas of natural flooding a common practice is to plant crops such as sorghum as the floodwater recede. Throughout the utilization of residual soil moisture the plant survives until the arrival of the rainy season. The plant matures with the onset of the rainy season and is harvested before the rising waters inundate the field.

3.4. Controlled Flood Irrigation.

This type of irrigation permits the regulation of the rise of floodwater to 5 cm per day for floating rice and 3 cm per day for paddy rice. In some area, small submersible dykes are built around plots to inhibit the rapid rise of flood

waters. With the application of more modern technology, dykes, canals, and sluice gates have been constructed to control and drain the water from perimeters and protect the crop from rice eating fish. Such a system provides greater reliability to the farmer for a successful crop.

3.5. Total Control.

The introduction of full water control systems throughout the construction of dams, dykes, canals, drains, and sluice gates provides a dependable supply of water and allows drainage of leveled plots. Both gravity flow systems and pump systems are found in the Sahel countries, but, because of management and social problems, they have never fulfilled expectations.

3.6. River Basin Development.

Currently, there is the development of interstate river basin authorities on the Senegal (OMVS), Gambia (OMVG), and Niger (NBA). A problem which may develop with the growth of the river basin authorities is the emphasis upon transportation and power generation to the detriment of irrigation.

4. Senegal.

In years of normal rainfall, cereal imports represent about one third of the country's needs (consumption 850 to

920,000 tons; imports 260 to 330,000 tons each year).
Imported cereals are mainly rice and wheat, (Ediafric, 1978).
In view of the large deficit, it is clear that every effort
must be made to free production from uncertainties due to
climatic variation in order to increase productivity. Large
scale irrigation extension is dependent upon the creation of
regulated storage on the Senegal, Gambia and Casamance rivers.
In the absence of such storage reservoirs, it has been
possible to develop only small areas of modern irrigated
agriculture.

The Government of Senegal has made a commitment to the
expansion of irrigation as a mean of increasing food
production. Agriculture is delegated to various regional
development organizations.

SAED is the largest organization which is responsible for
the development of irrigation in the Senegal River Valley. In
other areas agricultural development is under the direction of
various organizations which usually have a division that
oversees irrigation development. SOMIVAC, SODEFITEX, SODAGRI
have been created for the sole purpose of increasing cereals
production, especially rice, through the development of
irrigation. There are also smaller actions such as
"Groupements Villageois or Organisations Paysannes" backed by
Non-Governmental Organisations such as Peace Corps,
Volontaires du Progres, Terre des Hommes etc., where
development is at a smaller scale. All these institutions

have their own administration, extension study, and programming services.

The priority of the Government of Senegal is development. The irrigation perimeters have been in the development of large scale total water control systems. However, high development costs, difficulty in organizing farmers, and heavy recurrent costs plus a desire to decentralize management have resulted in a new interest in small-scale irrigation development.

The approach at present appears to be a continued effort to expand the total water control systems, especially in the Senegal River Valley (Fig.2) and also to provide support and assistance to small scale development wherever feasible. Irrigation development is located in five regions of Senegal: The Senegal River Valley, Delta area, Anambe Basin, Lower Casamance Region, and Niayes Region.

Irrigation has been practiced by many people and the prevalent systems in Senegal include:

(a) traditional hand watering

(b) natural flood irrigation

(c) total water control system.

The Senegal River Basin, which has the highest potential for irrigation development, lies within different climatic zones, resulting in extreme fluctuations in rainfall.

In the northern part of the Basin, the average annual rainfall of 300 mm is limited to the months of July through

September. In the southern portion of the Basin, the average annual rainfall of 2000 mm occurs from May until October. Annual variations in rainfall are also extreme, especially in lower reaches of the River. Variations in annual stream flow are great and reflect the variations in annual precipitation.

The seasonal characteristics of the rainfall determine the Senegal River's floodplain configuration, consisting of a single flood wave moving down the River. The floodplain is inundated annually between Bakel and St Louis. As the flood moves through the Middle Valley and Delta region, it becomes significantly altered as peak flows decrease due to floodplain storage, evaporation and infiltration losses. With the end of the annual rains, the flood gradually recedes. At the end of the dry season (April to mid-June), flows decrease during most years to approximately 10 cu m/sec. at Bakel.

The Lower Senegal Valley is seriously affected by soil and water table salinity mainly because of the drought in the Sahel Region during the last two decades. This salinity with chloride, sulphate, sodium and magnesium of ancient neutral marine origin interfered, later on, with potential acidity of the mangrove.

Agriculture is the most important activity in the region and rice is becoming the most dominant crop since the construction of two dams at Diama and Manantaly and the establishment of new irrigated perimeters. It is estimated that 250,000 hectares can be irrigated within the next decade.

The Diama Dam located in the Delta of the Senegal River is to prevent salt water intrusion in the river and to provide a fresh water supply for irrigation in the Delta area. Irrigation development in much of the delta could encounter problems involving salinity and drainage, with resulting costs for development and operation.

The Manantaly Dam is located about 1,200 km upstream from the Atlantic Ocean. It is designed to permit a year-round irrigation of 225,000 hectares of land between Manantaly and St. Louis and a year-round flow of 100 cu m/sec. in excess for irrigation and other requirements to provide water depths needed for navigation. The Dam should also provide the production of 800 gigawatt-hours per year of electricity.

Two major types of irrigation schemes have been implemented along the Senegal River since 1973: large and small scale irrigated perimeters. Both systems are served by pumping water from the Senegal River or one of its old channels.

4.1. Small-Scale Perimeters.

These perimeters are characterized by small areas of 15 to 20 hectares of heavy clay soil, an average of 20 hectares per village perimeter and 15 to 20 farmers. The perimeter is close enough to the River in order to facilitate the water pumping but at the same time should not be subject to flooding. Clearing, stumping, and construction are done

collectively by farmers but canal network design, pumping station construction, and equipment are financed by the government. Each individual farmer is responsible for the leveling and construction of his own plot.

Land preparation is done in June exclusively with traditional hand hoe or shovel and without pre-irrigation to soften the soil. Fertilizers and yield varieties are often used by farmers. The average yield lies between 3.5 to 5.0 tons per hectare.

4.2. Large-Scale Perimeters.

Large scale perimeters mainly located in the Delta area are characterized by an area between 100 to 10,000 hectares. Each perimeter is provided with heavy equipment (ie., tractors, combines) and large pumping stations (more than 240 hp). The perimeter is divided into holdings of 0.5 to 3.0 hectares each and is fed by a canal capable of irrigating 10 hectares.

The pumping stations and irrigation network are built and maintained by the government which also decides on the crop to be planted, the varieties to be grown and the agricultural calendar.

Land preparation, seeding, and threshing are done mechanically. Land preparation requires deep plowing every three to four years and offset and cross-harrowing in intervening years. Seeding is mechanized, but weeding and

harvesting are done manually. The main problem other than soil and ground water salinity is the scarcity of labor during the peak periods of the years, especially during the harvesting period.

The average yield is 2.5 tons of paddy rice per hectare. By mid 1977 SAED had brought 9600 hectares under irrigation in the Senegal valley and delta area. Since then, substantial progress has been made.

Under the direction of SODEFITEX and SODAGRI, there were in the late 1980s 10,000 hectares of modern irrigation systems in operation in eastern Senegal and Casamance. The irrigated perimeters are located mainly in the Anambe Basin. Water behind the Anambe Dam is distributed by gravity onto the rice fields by a well designed system of canals. The two main irrigated crops are rice and corn.

In the Niayes region, there are large quantities of subsurface water at relatively shallow depths. Traditional well gardening has been practiced for centuries, but reliance on wells has significantly increased since the drought of the early 1970s, particularly for the dry season. Farmers using traditional technology are usually able to produce between 25 to 40 tons/ha of vegetables. Although gardens vary greatly in size depending on factors such as cropping season, family size, recharge rate, depth of water table and amount of land in dryland crops, most plots are small, less than 1/10 to 1/3 hectares, with a minimum of one well for every 1,500 to 2,500

square meters.

5. Lower Casamance.

For many years, the Lower Casamance region was a food self-sufficient region. In recent decades, this region has experienced food deficits.

Because of the Sahelian drought during the last two decades, the annual amount of rainfall in the Casamance region has decreased from 1,500 mm to less than 1,000 mm. The most striking fact is that during the period from 1966-1980, there was greater than 20% reduction in rainfall, and over the period of 1980-1984 the average was even lower (Fig 3).

Since the Lower Casamance region is generally considered marginal for mangrove rice, a reduction of 20 to 30% in rainfall has been even more disastrous for yields. With insufficient rainfall, there is inadequate leaching of the polders and as the salt level increases the production of rice becomes nearly impossible.

Geographically, the saline portion of the Casamance River estuary extends 220 km into the country; salt water regularly rises as far as 130 km inland. Salt content reaches its maximum level in June and its minimum level in October. The salinity at Ziguinchor varies between 19 and 37 grams of salt per liter.

Apart from the Casamance River, there are 5 major basins in the Lower Casamance. All of them are subject to the sea

Rice Production
Bignona (North)
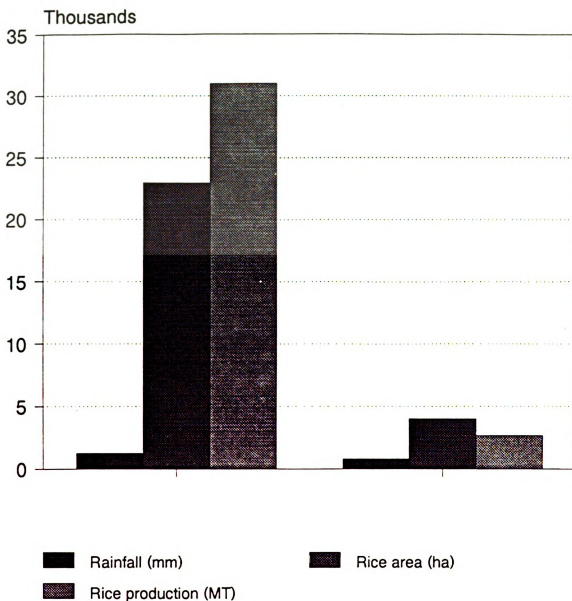
Figure 3. Evolution of rice production in Lower Casamance.

water effects of the river, and the maximum amplitude of the tide is approximately one meter. Since the topography of the region is quite flat, all of the backwaters (marigots and bolons) are also affected by salt over much of their length.

Another result of the level landscape is a lack of runoff in the watershed. On average, only 6% of rainfall in the Lower Casamance goes into runoff (Harza Engineering, 1981) and thereby helping to leach mangrove rice fields. Given the shortage of rainfall over the last several years and the increasing accumulation of salt, the number of abandoned mangrove rice fields is multiplying all over the Casamance Region.

Along the tidal portions of the river basins, we can observe not only a tendency towards increased salinity of the river bed itself, but also a serious tendency toward increased salinity of the underlying water table.

This salinization process occurs at the end of the rainy season as a result of high tides, hence feeding the water table. Consequently, not only the polders, but also the rice fields located on the first level of terraces are affected by the rainfall shortage and the problem of salinization.

Irrigation and drainage have been practiced in the Lower Casamance by farmers for centuries. The traditional Diola system for reclaiming mangroves is based on the judicious use of the movements of the tide. In the absence of free water, farmers managed to leach the salt from their fields without

lowering the pH. This result was obtained by allowing a continual readmission of salt water during the dry season. In years of abundant rainfall, this type of field can produce as much as 3 tons of paddy, rice per hectare with no fertilizer and, in many cases, no weeding. The double dyke system, which makes it possible to tap all the resources of the mangrove (wood, charcoal, fish, pasturage, rice farming), is well adapted but requires a great deal of labor. Given the last 15 years of low rainfall and the flight of young people toward the cities, the future of mangrove rice cultivation is in question (Schillinger, 1978).

Site development (polders, drains, anti-salt dams) in the Lower casamance focuses on the desalinization of the soil by means of fresh water retention and partial exclusion of brackish water. The difficulty encountered in these systems involves finding a reasonable balance between the exclusion of saline water and the drying out of the soil, which may provoke a drastic decline in pH.

The low level of rainfall in recent years has dramatically reduced the amount of fresh water available for leaching the salt out of these fields, thus diminishing the benefits of site development.

Nevertheless, after monitoring the Medina polder for five years, Beye (1977) was able to reach some very important conclusions:

(a) for the polders which were gravity drained, the

shallow drainage system spaced at a distance of 20 m (57% clay) and blocking the entry of brackish water resulted in the leaching of 50% of the salt in the upper layer (0-20 cm deep). Unfortunately, in years of little rainfall, the salt content in the polders quickly rose again.

(b) with respect to the pH level, the drainage system allowing the entry of saline water every 5 days during the off-season in order to avoid total drying out of the soil proved to be the best. The pH held steady around 6.5.

These results and those obtained by Marius and Cheval (1980) at Tobor and Guidel show that site development (drainage) converts the surface horizons from acid sulfate soil to a para-acid sulfate soil and, with more fresh water (greater rainfall levels, fresh water retention dykes), the polders could become viable for rice production. That is why the Government of Senegal has recently started up an important soil and water conservation program in Casamance in order to improve rice production in the region. The construction of small anti-salt dams in most of the valleys remains the primary objective.

It is estimated that a total of 100,000 hectares could be irrigated in the Casamance area and the planned growth is 3,000 hectares per year. Most of the potential for irrigation is located in the Lower Casamance region along the main

tributaries: Bignona: 12,000 hectares, Baila: 34,000 hectares, Kamobeul: 32,000 hectares and, Guidel: 1,500 hectares.

Unlike the National Programs of Soil and Water Conservation, which are designed for large watersheds of several hundreds of square kilometers, and sophisticated water control systems, the small anti-salt dams are built and managed by peasants of one, or, at the very most, a group of three villages. These programs are less ambitious and directed towards small watersheds not larger than several hundreds of hectares. Most of the rice fields are not strongly affected by the salt. The main problem encountered there is keeping a sufficient depth of water in the plots during the whole growing season.

The anti-salt dam consists of a dyke and one or two reinforced concrete structures. The dyke is 400 to 1,000 meters long, 4 to 6 meters wide at the bottom, and 2 to 4 meters on the top. The height varies between 1.5 to 2.5 meters. In many cases, the dyke is built entirely by the farmers of one, or at the very most 3, villages which share the land on both sides of the dam. In general a road which crosses the entire watershed is used as a foundation. This may also present the advantage of facilitating the access to many villages during the rainy season, mainly during the floods.

The reinforced concrete structure located in the affluent

bed, consists of two or four gates (1.5 meter wide); each of which is designed to have a rectangular weir 20 centimeters high and 60 centimeters wide at the bottom.

In order to retain water behind the dam, the peasants must close the gates by installing two lines of planks on the weir, and fill the spaces between them with mud. The planks are placed one on top of the other. The number of planks depends only on the farming calendar. Each plank is 20 centimeters in height and slightly longer than the gate width.

At the beginning of the rainy season, farmers put in place two or three planks to retain a certain amount of water which will inundate the lowest rice fields and dissolve the salt. Water will then be flushed out by removing the planks. This type of operation has to be done as many times as needed to get good conditions for growing rice, in many cases, until mid-July when they start plowing their plots.

After the rice transplanting operation, which begins mid-August, farmers put in place more planks in order to retain more water as the rainy season ends. Only after big storms is excess water released to avoid flooding the plants. During the dry season, the gates remain closed; sea water is not admitted.

Because of a poor water management program behind the anti-salt dams, many conflicts have arisen between farmers throughout the entire Lower Casamance. The rice fields close to the dams are flooded too fast because of their lower

position on the toposequence, especially at a time when the
plants are not robust enough to support a long submersion.
During the same period of time the rice fields located at the
terraces need a certain depth of water to maintain good
conditions for rice growth.

In accordance with the location of their plots on the
toposequence, farmers decide whether or not to release a part
of the water stored in the reservoir. Often, there is no
agreement among landowners, or a final decision is made too
late. Sometimes the problem of how much water to release from
the reservoir can be more complicated, as in when paddy fields
downstream from the dams do not get enough water to leach the
salt out.
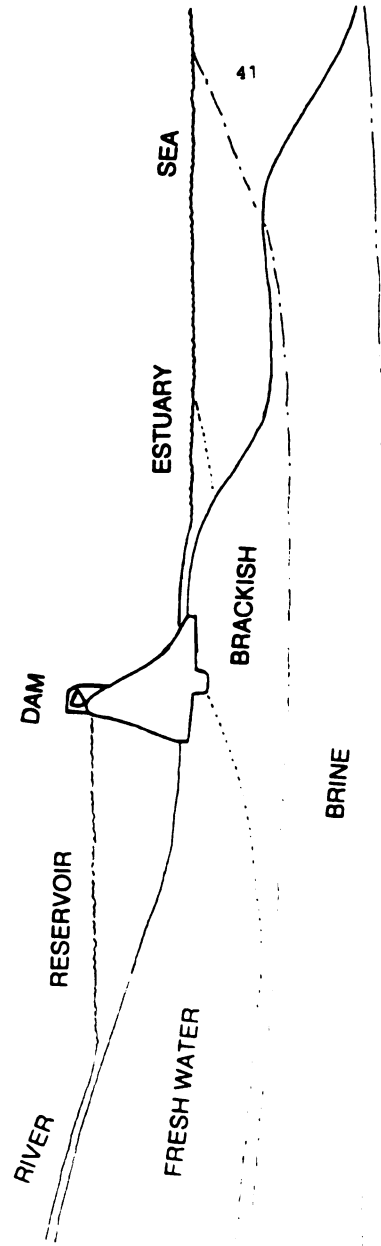
Figure 4. Typical toposequence in Lower Casamance.

B. HYDRAULICS OF GROUNDWATER AND SOLUTE TRANSPORT.

The term groundwater is usually reserved for the subsurface water, which occurs beneath the water table in soils and geological formations that are fully saturated.

Groundwater constitutes an important component of water resource systems, supplying water for domestic use, industry, and agriculture.

1. Equations of Groundwater Flow.

The basic law of flow is Darcy's law. It is valid for groundwater flow in any direction in space, and is stated as follows:

$$Q = -KA \frac{dh}{dl} \qquad (1)$$

$$v = \frac{Q}{A} = -K \frac{dh}{dl} \qquad (2)$$

where:

K = hydraulic conductivity or coefficient of permeability [L/T]

42

Q = volume flux or flow rate [L³/T]

A = cross section [L²]

v = specific discharge [L/T]

dh/dl = hydraulic gradient [L/L]

When combined with the continuity equation, a partial differential equation is the result for:

        (a) steady-state saturated flow,

        (b) transient saturated flow,

1.1. Steady –State Saturated Flow.

Consider a unit volume of porous media such as that shown in (Fig.5). Such an element is called an elemental control volume. The law of conservation of mass for steady-state flow through porous medium requires that the rate of flow into an elemental control volume be equal to the rate of fluid mass flows out of any elemental control volume. The equation of continuity that translates this law into mathematical form can be written, with reference to (Fig.5), as:

$$-\frac{\partial(\rho v_x)}{\partial x} - \frac{\partial(\rho v_y)}{\partial y} - \frac{\partial(\rho v_z)}{\partial z} = 0 \qquad (3)$$

where ρ is the fluid density.
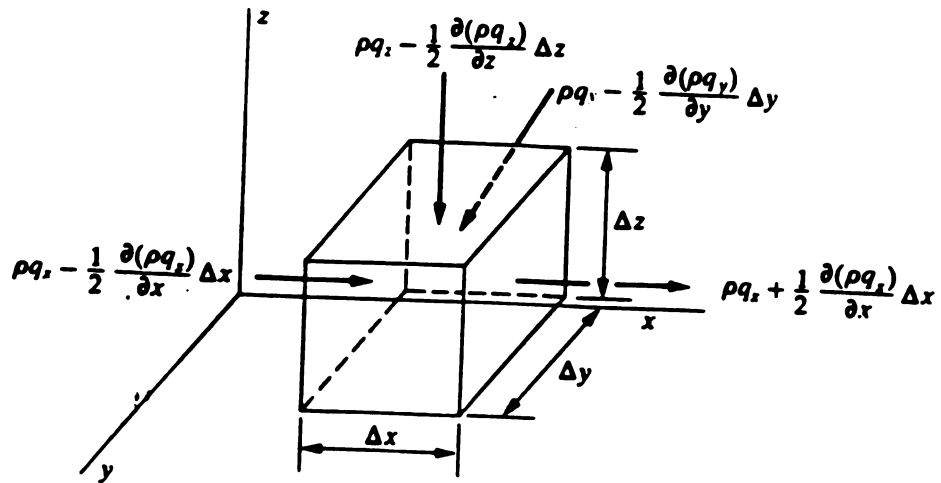
Figure. 5. Mass fluxes in a unit volume of saturated soil:
After Gray (1973).

If the fluid is incompressible, $\rho(x,y,z)$ is constant and the ρ's can be removed from Eq.(3). Even if the fluid is compressible and $\rho(x, y, z)$ is not constant, it can be shown that terms in the form $\rho \partial v_x /\partial x$ are much greater than terms in the form $v_x \partial \rho/\partial x$ both of which arise when the chain rule is used to expand Eq.(3). In either case, Eq.(3) simplifies to:

$$-\frac{\partial v_x}{\partial x} - \frac{\partial v_y}{\partial y} - \frac{\partial v_z}{\partial z} = 0 \tag{4}$$

Substitution of Darcy's law for v_x, v_y, and v_z in Eq.(4) yields the equation of flow through an anisotropic saturated porous media:

$$\frac{\partial}{\partial x}(K_x \frac{\partial h}{\partial x}) + \frac{\partial}{\partial y}(K_y \frac{\partial h}{\partial y}) + \frac{\partial}{\partial z}(K_z \frac{\partial h}{\partial z}) = 0 \tag{5}$$

For isotropic media, $K_x = K_y = K_z$; if the media is also homogeneous, then $K(x,y,z)$ is constant. Equation (5) then reduces to the equation of flow for steady-state flow through a homogeneous, isotropic media:

$$\frac{\partial^2 h}{\partial x^2} + \frac{\partial^2 h}{\partial y^2} + \frac{\partial^2 h}{\partial z^2} = 0 \qquad (6)$$

Equation (6) is known as Laplace's equation. Its solution is a function of h in terms of x, y, and z that describes the value of the hydraulic head (h) at any point in a three-dimensional flow field. A solution to Eq.(6) allows us to produce a contoured equipotential map of h and, with the addition of flowlines, a flow net.

In a two-dimensional flow field, for example, in the xz-plane, the central term of Eq.(6) would drop out and the solution would be a function of h in terms of x and z (ie., h(x,z)).

1.2. Transient Saturated Flow.

The law of conservation of mass for transient flow in a saturated porous medium requires that the net rate of fluid mass flow into an elemental control volume be equal to the time rate of change of fluid mass storage within the element. With reference to (Fig.3), the equation of continuity takes the form:

$$-\frac{\partial (\rho v_x)}{\partial x} - \frac{\partial (\rho v_y)}{\partial y} - \frac{\partial \rho v_z)}{\partial z} = \frac{\partial (\rho n)}{\partial t} \qquad (7)$$

where n is the porosity of the aquifer.

Expanding the right hand side, Eq. (7) is:

$$-\frac{\partial(\rho v_x)}{\partial x}-\frac{\partial(\rho v_y)}{\partial y}-\frac{\partial(\rho v_z)}{\partial z}=n\frac{\partial\rho}{\partial t}+\rho\frac{\partial n}{\partial t} \qquad (8)$$

The first term on the right-hand side of Eq.(8) is the mass rate of water produced by an expansion of the water under a change in its density ρ. The second term is the mass rate of water produced by compaction of the porous medium as reflected by the change in its porosity n. The first term is controlled by the compressibility of the fluid β and the second term by the compressibility of the aquifer α. The change in ρ and the change in n are both produced by a change in h, and the volume of water produced by the two mechanisms for a unit decline in head is S_s, where S_s is the specific storage given by $S_s = g(\alpha + \beta n)$. The mass rate of water produced (time rate of change of fluid mass storage) is S_s $\partial h/\partial t$, and Eq.(8) becomes:

$$-\frac{\partial(\rho v_x)}{\partial x}-\frac{\partial(\rho v_y)}{\partial y}-\frac{\partial(\rho v_z)}{\partial z}=\rho S_s\frac{\partial h}{\partial t} \qquad (9)$$

Expanding the terms on the left-hand side by the chain rule and recognizing that terms of the form $\rho \partial v_x / \partial x$ are much greater than terms of the form $v_x \partial \rho / \partial x$ allows us to eliminate ρ from both sides of Eq.(9). Inserting Darcy's law we obtain:

$$\frac{\partial}{\partial x}(K_x \frac{\partial h}{\partial x}) + \frac{\partial}{\partial y}(K_y \frac{\partial h}{\partial y}) + \frac{\partial}{\partial z}(K_z \frac{\partial h}{\partial z}) = S_s \frac{\partial h}{\partial t} \qquad (10)$$

This is the equation of flow for transient flow through a saturated anisotropic porous medium. If the medium is homogeneous and isotropic, Eq.(10) reduces to:

$$\frac{\partial^2 h}{\partial x^2} + \frac{\partial^2 h}{\partial y^2} + \frac{\partial^2 h}{\partial z^2} = \frac{S_s}{K}\frac{\partial h}{\partial t} \qquad (11)$$

or, expanding S_s:

$$\frac{\partial^2 h}{\partial x^2} + \frac{\partial^2 h}{\partial y^2} + \frac{\partial^2 h}{\partial z^2} = \frac{\rho g(\alpha + n\beta)}{K}\frac{\partial h}{\partial t} \qquad (12)$$

Equation (12) is known as the diffusion equation. The solution h(x,y,z,t) describes the value of the hydraulic head at any point in a flow field at any time. A solution requires knowledge of the three basic hydrogeological parameters, K, α, and n, and the fluid parameters, α and β.

For the special case of a horizontally bounded aquifer of thickness b, S = S,b and T = Kb, and the two-dimensional form of equation (12) becomes:

$$\frac{\partial^2 h}{\partial x^2} + \frac{\partial^2 h}{\partial y^2} = \frac{S}{T}\frac{\partial h}{\partial t} \qquad (13)$$

The solution h(x,y,t) describes the hydraulic head at any point on a horizontal plane through the horizontal aquifer at any time. This solution requires knowledge of the aquifer parameters S and T.

For the special case of a horizontally unbounded aquifer (Phreatic Aquifer), T = Kb, where b is the aquifer saturated thickness, and S_y the specific yield. S_y is defined as the volume of water, an unconfined aquifer releases from storage per unit area of aquifer per unit decline in water table.

$S_y = n_e$, where n_e is the effective porosity of the aquifer.

The technique of analysis of groundwater flow is a four-

step process, involving:

1. examination of the physical problem,

2. replacement of the physical problem by an
   equivalent mathematical expression,

3. solution of the mathematical problem with the accepted
   techniques of mathematics,

4. interpretation of the mathematical results in terms of
   the physical problem.

Mathematical models based on the physics of flow usually take the form of boundary-value problems. To fully define a transient boundary-value problem for subsurface flow we need to know:

1. the size and shape of the region of flow,

2. the equation of flow within the region,

3. the boundary conditions around the boundaries of the
   region,

4. the initial conditions in the region,

5. the spatial distribution of the hydrogeologic
   parameters that control the flow,

6. a mathematical method of solution.

If the boundary-value problem is for a steady-state system, requirement (4) is removed.

The method of solution can be categorized roughly into five approaches:

1. solution by inspection,

2. solution by graphical techniques,

3. solution by analog model,

4. solution by analytical mathematical techniques,

5. solution by numerical mathematical techniques.

2. Solute Transport.

The common starting point in the development of differential equations to describe the transport of solutes in porous materials is to consider the flux of solute into and out of a fixed elemental volume within the flow domain. The physical processes that control the flux into and out of the elemental volume are advection and hydrodynamic dispersion. Loss or gain of solute mass in the elemental volume can occur as a result of chemical or biochemical reactions or radioactive decay.

Advection is the component of solute movement attributed to transport by the flowing groundwater. The rate of transport is equal to the average linear velocity, v, where $v = v/n$, v being the specific discharge or Darcy's velocity, and n the porosity.

Hydrodynamic dispersion, or spreading phenomena, is an irreversible process. It can be a mechanical dispersion which dominates at a high velocity or a diffusion at a very low

velocity. However, in many cases, or as a first approximation, the fluxes due to hydrodynamic dispersion are much smaller than those due to advection, for example, for saturated flow:

$$| qc | > | nD_h \cdot \nabla c |$$

(14)

where: c = solute concentration [M/L^3]

q = total flux [L^3/L^{2}T]

n = porosity

D$_h$ = hydrodynamic dispersion coefficient [L^2/T].

Under such conditions, polluted groundwater bodies move in the aquifer along the pathlines of the water itself, at the velocity of the latter. In the absence of adsorption, sources, and sinks, the pollutant balanced equation for saturated flow, θ=n , reduces to:

$$\frac{\partial nc}{\partial t} = -\nabla \cdot cq$$

(15)

$$q = nv$$

For the simple case of a homogeneous nondeformable porous

medium $\mathbf{v}n = 0$, and $\partial n/\partial t = 0$, Eq.(15) reduces to:

$$\frac{\partial c}{\partial t} = v \cdot \nabla c - c \nabla \cdot v \qquad\qquad (16)$$

For steady flow of an incompressible fluid in a homogeneous nondeformable porous medium, $\mathbf{v}.V = 0$, Eq.(16) becomes:

$$\frac{\partial c}{\partial t} = -v \cdot \nabla c \qquad\qquad (17)$$

In a two-dimensional flow in the xy-plane, Eq(17) takes the form:

$$\frac{\partial c}{\partial t} = -v_x \frac{\partial c}{\partial x} - v_y \frac{\partial c}{\partial y} \qquad\qquad (18)$$

The solution of Eq.(18) which is a linear hyperbolic partial-differential equation in the three independent variables (x, y, t), can be rewritten in the form:

$$\frac{\partial c}{\partial t} = \frac{\partial c}{\partial t} + v_x \frac{\partial c}{\partial t} + v_y \frac{\partial c}{\partial t} \qquad (19)$$

It can be represented, at least in principle, by lines of constant concentration, called characteristics. Along such a characteristic, the variation of c vanishes:

$$dc = \frac{\partial c}{\partial t} dt + \frac{\partial c}{\partial x} dx + \frac{\partial c}{\partial y} dy = 0 \qquad (20)$$

The statement dc/dt = 0 means that the concentration of an observed fixed particle does not change with time as it travels in the considered domain. For the above reason, dx = V_x dt, and dy = V_y dt. This means that the direction of the characteristic coincides with that of the flow, namely that of the streamline.

Similar to the models of saturated flow problems, the complete model of a pollution problem consists of the following items:

1. specification of the geometrical configuration of the closed surface that bounds the problem area with possible segments at infinity,

2. specification of the dependent variables of the

pollution problem (i.e., the concentration, $c(x,t)$) of the specific constituent or constituents under consideration.

III. RESEARCH METHODOLOGY

A. RESEARCH APPROACH.

Based upon the need for an improved understanding of the engineering and management aspects of the anti-salt dams, the following approaches are proposed for achieving the objectives of this research:

Objective: 1. To study the groundwater flow and quality in a typical valley of the Lower Casamance region.

The approach to be followed under this objective will be to describe and measure the groundwater flow and quality of a typical valley in the Lower Casamance region in Senegal. For this study, the Katoure valley will be used because of the availability of hydrologic and soils data. Field data have been collected for more than six years.

Objective: 2. To develop a groundwater simulation model for evaluating water movement in the aquifer.

The approach to be used under this objective will be to develop a finite element model for evaluating groundwater movement in a mono layered aquifer. Data from the Katoure valley site will be used to verify the model.

Objective: 3. To evaluate improved management strategies for irrigation behind anti-salt dams.

An evaluation and discussion of the results of the simulation model will be made so that recommendations for improved management parameters can be formulated.

B. **EXPERIMENTAL METHODS.**

1. **Site Description.**

The Katoure site is located 5 km Southwest of Ziguinchor (Fig. 6). The watershed area is about 95.6 square kilometers (BCEOM - IRAT 1970). The Katoure river is an affluent of the Kamoubeul River which itself is the most important affluent of the Casamance River.

1.1. **Climate and Hydrology.**

Like the whole sub-humid west African region, the climate is sub-Guinean characterized by two distinct seasons:

1. a dry season from November to May,

2. a rainy season which extends from June to October.

The average rainfall in Ziguinchor prior to 1965 measured around 1,600 mm. Seventy percent of the time the highest total monthly rainfall (one third of the annual total) was recorded in the month of August, 20 percent of the time in September, and 10 percent of the time in July. The calculated

potential evapotranspiration (class A pan) is about 1,300 mm per year at Ziguinchor.

During the rainy season the water balance prepared by Schillinger (1978) shows a major surplus only during the months of July, August, and September. Beginning in October, periods of drought appear frequently creating a negative balance.

Because of its very low relief and current rainfall deficit, the hydrology of the watershed is under the influence of the sea water intrusion. Salt water frequently flows as far as 30 km from the confluence of the Katoure River, creating an acute salinization problem in the rice fields located on the river plain. Above the river plain we have areas which are fed by run off coming from the plateau and a rise of the water table. During the period from August 15 to October 1, these soils often benefit from the underground water, which gives local rice cultivation a particular character.

1.2. Soil.

The nature of the soils depends on the soil's position in the topographical sequence.

On the plateau, the soil is sandy loam with a sandy surface. Two types predominate:
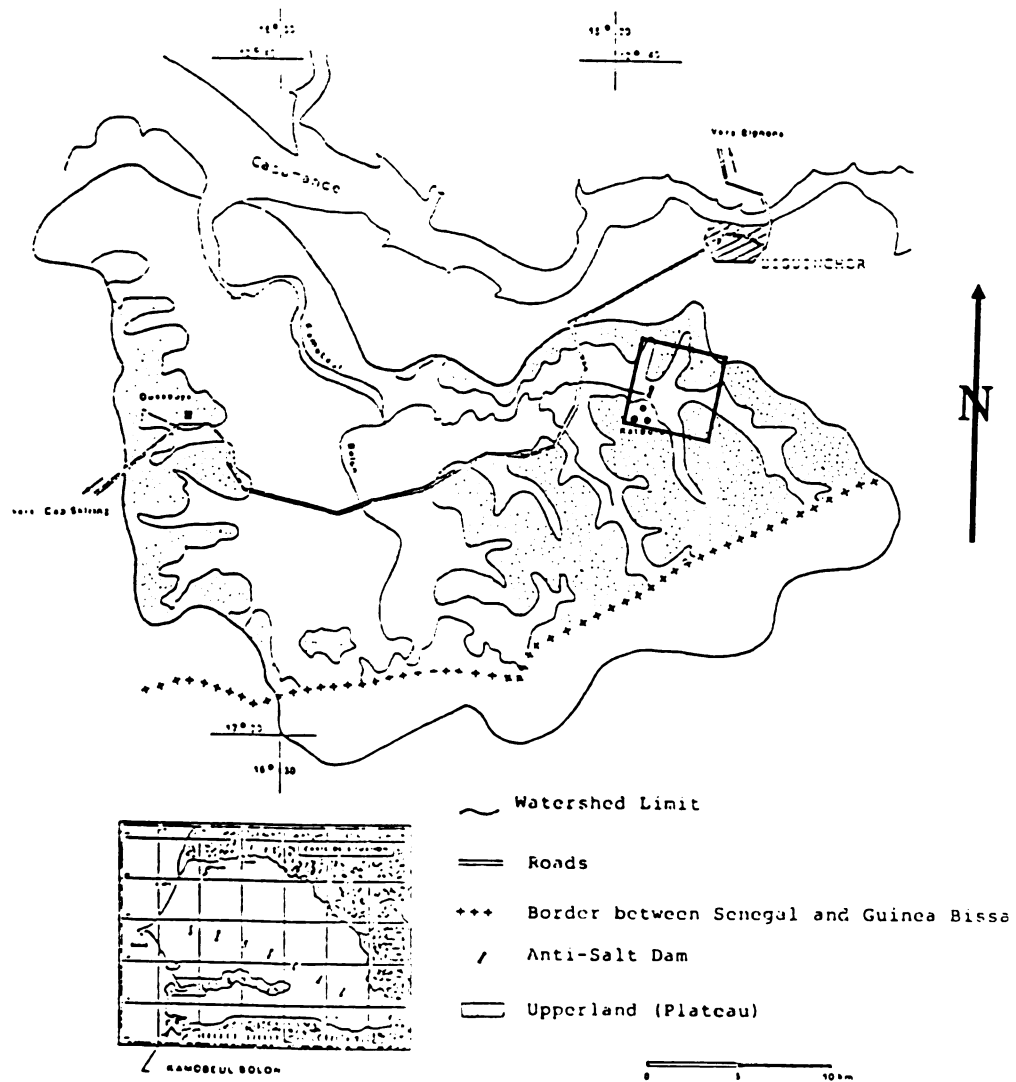
Figure 6. Map of the Kamoubeul River's watershed

    (a)   red, low base status iron soil with a higher clay content in the B horizon,

    (b)   ferrugineous, leached tropical beige soils found in the central well drained uplands.

Along the inland valley and the river itself, there can be found a sandy zone (50 to 80% sand) that is temporally flooded during the rainy season. The dominant types are the Gray water-bearing soils, well known as transition soils between the plateau and the alluvial plain.

The upstream portion of these soils is often abandoned because underground water no longer rises to the same level after more than 10 years of drought. The middle portion is used occasionally for rice cultivation of direct seeded rice; the lower portion, which includes the fringes of the alluvial plain, is also used for rice, either by direct seeding or by transplanting.

The inland valley is dominated by mineral hydromophic soils, characterized by a fine texture (48% clay) and high, natural fertility. These soils, located upstream of the alluvial plain, are not affected by the salinity problem. They are often surrounded by a sandy upper terrace of 0.5 to 1 meter in altitude above the average level of the river, while the altitude of the upper terraces ranges between 2 to 6 meters.

The alluvial plain is mainly dominated by two types of soil, both affected by salinity and acidity problems:

(a) para-acid sulfate soils which can be classified as Loamy-clayey acid soils,

(b) acid sulfate soil which contains 80% sand.

Both types of soils are the result of alluvial infilling which followed the great Ogolian regression, and plateau colluvium.

1.3. Experimental Network.

The Katoure Dam is 440 meters long and designed to protect 780 hectares against the intrusion of saline water during the daily tides. It is located next to the village of Katoure, 15 km from the mouth of the river. The dike was entirely built by farmers of three villages who own lands in the valley. The dike is 440 meters long, 2.60 meters wide on the top, 5.0 meters at the bottom, and the average height is about 1.5 meters.

A reinforced concrete structure with four gates is built in the river bed. Each gate is 1.50 meters wide and designed with a rectangular weir.

A network of 98 piezometers was installed on 100 hectares located on both sides of the dam; 80 hectares behind the dam and 20 hectares upstream (Fig.7). The depth of the

piezometers varies between 6.0 and 12.0 meters.

2. Piezometric Tests

Two methods have been used in order to determine the hydraulic conductivity of the aquifer.

    (a)   The LeFranc Test, named after a French geologist, is based on the realization of a permanent flow regime. This test is a variant of the absorption test. This test has been done on 98 piezometers.

    (b)   The Slug Test has been performed on 42 piezometers in order to validate the results of the previous test.

2.1. Principle of LeFranc Test

This test consists of creating a variation of head either by injection or by pumping into a cavity with a known diameter. A pipe screened on one end is introduced to the cavity. The screened part of the pipe is 1.5 meters long and should be entirely located under the watertable.

From a tank, water is poured into the piezometer through a length of rubber tubing (Fig.8). The overflow is collected in a beaker. A quasi permanent flow regime is reached when the difference between the volume of water from the tank and the overflow becomes constant over a period of time.
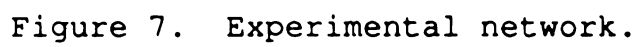
Figure 7. Experimental network.

Then, the inflow water is stopped and the drawdown measured every 15 seconds during the first 20 minutes and every 5 minutes during the next 40 minutes.

The LeFranc test does not estimate a local permeability but an overall value, which can be very different. Nevertheless, it is a quick and cheap test which can be easily repeated , and it gives important indications with regard to aquifer structure and heterogeneity.

The mathematical resolution of this type of problem is done by Maurice Cassan (Les Essais d'Eau dans la Reconnaissance des Sols). The physical formulation of the problem is as follows.

Let H be the depth of water in the tube above the watertable, and Z the depth of water at any time t. For an interval of time dt the drawdown is dz and the flow can be expressed by the following equation:

$$Q = \frac{A dz}{dt}$$

(21)

where A is the internal cross-section of the pipe, and dz/dt = infiltration rate.

The negative sign means that any change on dz implies a head reduction.

Because the intake is long and cylindrical, it is recommended to use the coordinates of an ellipsoid with a focal distance equal to 1/2.

Thus Q = mKD, and equating with equation (21), we obtain:

$$-\frac{Adz}{dt} = mKD \tag{22}$$

where D = internal diameter of the pipe

K = hydraulic conductivity of the aquifer

m = shape coefficient. If 1/D > 10 then

m = (2 π 1/D) / ln(2 1/D)

1 = length of the screened portion of the pipe

At t = 0, Z = H and integrating (22), we obtain:

$$\int \frac{dz}{Z} = -\frac{mKD}{A} \int dt \tag{23}$$

$$\ln Z = -\frac{MKD}{A} t + Constant \tag{24}$$
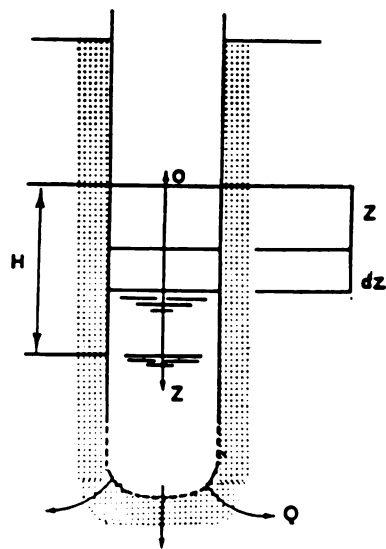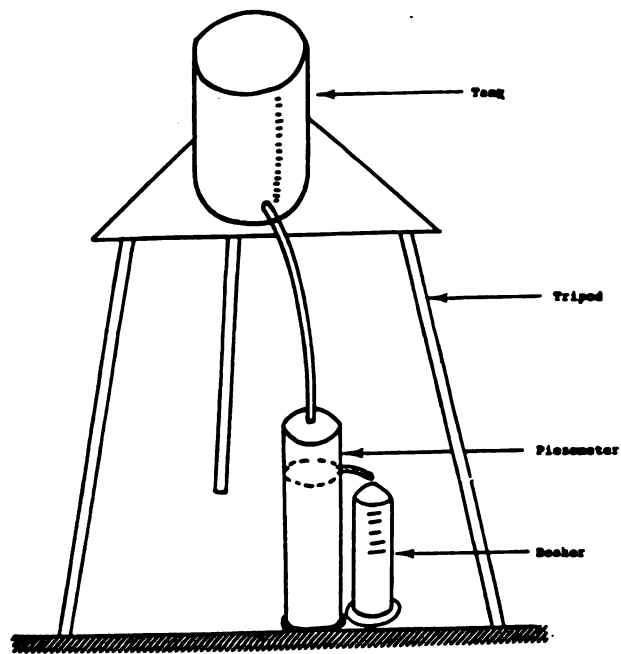
Figure 8. Apparatus for LeFranc test.

ln H = Constant.

$$\ln Z = -\frac{MKD}{A}t + \ln H \tag{25}$$

$$\ln Z - \ln H = -\frac{mKD}{A}t \tag{26}$$

$$\ln\frac{Z}{H} = -\frac{mKD}{A}t \tag{27}$$

$$\frac{Z}{H} = e^{-\frac{mKD}{A}t} \tag{28}$$

$$Z = He^{-\frac{mKD}{A}t} \tag{29}$$

By using $\log_{10}$ instead of ln, equation (29) becomes:

$$2.3\log\frac{Z}{H} = -\frac{mKD}{A}t \tag{30}$$

$$t = -\frac{2.3A}{mKD} \log \frac{Z}{H} \tag{31}$$

where A is the internal cross section of the pipe. It is also assumed to be equal to the cross section of the cavity.

$$A = \frac{\pi D^2}{4} \tag{32}$$

Equation (32) becomes:

$$t = -\frac{2.3\pi D}{4mK} \log \frac{Z}{H} \tag{33}$$

If we plot in a semi log scale Z/H function of time, t, we obtain a straight line with a negative slope(s)

$$s = \frac{2.3\pi D}{4mK} \tag{34}$$

The hydraulic conductivity (K) is then computed as

follows:

$$K = \frac{2.3\pi D}{4sm}$$
(35)

2.2. Principle of Slug Test.

The method is initiated by causing an instantaneous change in the water level in a piezometer through a sudden introduction of a known volume of water or by introducing a solid cylinder of known volume into the piezometer. The recovery of the water level with time is then observed. The simplest interpretation of piezometer-recovery data is that of Hvorslev (1951). His initial analysis assumed a homogeneous, isotropic, finite medium in which both soil and water are incompressible.

The rate of inflow, q, at the piezometer tip at any time, t, is proportional to the hydraulic conductivity, K, and to the unrecovered head difference, H - h, so that

$$q(t) = \pi r^2 \frac{dh}{dt} = FK(H-h)$$
(36)

where F is a factor that depends on the shape and the

dimensions of the piezometer intake.

Hvorslev defines the basic time lag, T_0, as:

$$T_0 = \frac{\pi r^2}{FK} \tag{37}$$

When this parameter is substituted in Eq.(37), the solution to the resulting ordinary differential equation, with the initial condition, $h = H_0$ at $t = 0$, is:

$$\frac{H-h}{H-h} = e^{-t/T_0} \tag{38}$$

To interpret a set of field recovery data, the data are plotted and the value of T_0 measured graphically. K is determined from Eq.(38). For a piezometer intake of length L and radius R, with L/R > 8, Hvorslev (1951) has evaluated the shape factor, F. The resulting expression for K is:

$$K = \frac{r^2 \ln(L/R)}{2LT_0} \tag{39}$$

For slug tests run in piezometers that are open over the entire thickness of a confined aquifer, Cooper et al. (1967) and Papadopoulos et al. (1973) have evolved a test-interpretation procedure. Their analysis is subject to the same assumptions as the Theis solution for pumpage from a confined aquifer. Contrary to the Hvorslev method of analysis, it includes consideration of both formation and water compressibility. It utilizes a curve-matching procedure to determine the aquifer coefficients T and S. The hydraulic conductivity K can then be determined on the basis of the relation, K = T/b. Like the Theis solution, the method is based on the solution to a boundary-value problem that involves the transient equation flow, Eq.(13).

Both techniques presented are quite similar in principle and are easy to apply on field. However, they are heavily dependent on a high-quality piezometer intake. If the wellpoint or screen is corroded or clogged, measured values may be highly inaccurate. On the other hand, if a piezometer is developed by surging or backwashing prior to testing, the measured values may reflect the increased conductivities in the artificially induced gravel pack around the intake.

2.3. Field Data collection.

Piezometric heads were measured with an electrical device

every two weeks during the dry season from November to May and after every major storm during the rainy season. The estimated error of the device is about 2 centimeters.

Samples of surface and subsurface water were regularly analyzed (once per month) in order to determine the electrical conductivity (salinity), pH, and Aluminum sulfates, which are responsible for most of the acidity problems encountered in mangrove lands.

Besides the field tests described earlier, samples of the aquifer material at the location of each piezometer were analyzed for physical and chemical properties. Soil samples were taken from every one meter below the water table surface to a depth of six meters.

2.4. Data analysis

The major task of the analysis was the estimation of the average area and the optimal contouring of certain parameters such as piezometric heads, groundwater salinity, hydraulic conductivity.

The estimation problem becomes strongly significant because of the spatial variability of some soil physical parameters, the existence of a correlation structure, and the fact that the data contain errors in measurement since they were collected at unequally spaced intervals.

The method of estimation of random fields that was used is the so-called universal Kriging or nonstationary fields.

This method deals with estimating values of a field parameter or linear functions of the field at a point (or points) from a limited set of observed values.

Nonstationary is here limited to those cases where the mean cannot be assumed constant, and it becomes necessary to describe and account for the mean function m(u) in some manner. An unknown nonstationary drift also implies that the covariogram, whether semivariogram or covariance, cannot be estimated since the residuals are unknown. Hence, estimating the mean and estimating the covariogram are related processes. Universal Kriging proposes a particular functional form for modelling the mean and treats the related processes of mean and covariogram estimation as:

1) an iterative procedure estimating first one statistic, then the other,

2) an invocation of the theory of intrinsic random function of order k.

Developed by Matheron and others at the Fontainebleau School (1971), universal Kriging proposes that the mean (or drift) can be modeled as a linear combination of v basic functions f^n as follows:

$$m(u) = \sum_{n=0}^{v} v a_n f^n(u) \tag{40}$$

The basic functions are known functions, but the coefficients, a_n, where $n = 0,1,2,\ldots,v$ are unknown and have to be estimated. The iterative procedure involves finding the best unbiased linear estimate of the coefficients, a_n, of the drift by first assuming some covariogram structure, then forming the residuals from the estimated drift in an attempt to reconstitute the original assumed covariogram. The solution is obtained when the initial assumed covariogram and the reconstituted covariogram agree.

In the present case study, the experiment consisted of Kriging each observation point using neighboring points and then using various measures of the difference between kriged and known values as criteria for assessing the validity of the assumed underlying drift and covariogram model. The original data consisted of piezometric heads, salinity and pH of water samples taken from each piezometer, and hydraulic conductivity of the aquifer. Contoured maps of water table surface and salinity are drawn and used to evaluate groundwater flow and quality.

C. COMPUTER SIMULATION.

1. Groundwater Flow and Solute Transport Simulation

The numerical method used to simulate both groundwater flow and solute transport was the finite element method. This method is applied to the time dependent flow of a confined and isotropic aquifer, Eq (13). The same equation was used to solve for a phreatic aquifer assuming that the Dupuit assumption holds. A new term I is added to the general formula in order to account for infiltration. The general formula then becomes:

$$S\frac{\partial \phi}{\partial t} = \frac{\partial}{\partial x}(T\frac{\partial \phi}{\partial x}) + \frac{\partial}{\partial y}(T\frac{\partial \phi}{\partial y}) + I \qquad (41)$$

where S denotes the storativity or specific yield depending on whether or not the aquifer is confined, and I denotes the net infiltration or evaporation. The assumption was made that there is no leakage and that the boundary conditions are assumed to be of the first or second kind. Thus, everywhere along the boundary, either the head or the rate of water supply is given. Unlike the steady flow case, $\partial \phi/\partial t = 0$, initial conditions are needed. The initial condition at time t = 0 was $\phi = \phi^0 (x,y)$, where $\phi^0 (x,y)$ is a known function.

Equation (42) may be satisfied throughout a specified region R in the x-y plane. Boundary conditions must be satisfied on the boundary of that region. A general formulation of the boundary conditions can be written as

$$\phi = f \qquad (42)$$

and

$$T\frac{\partial \phi}{\partial n} = qh \qquad (43)$$

on S_1 and S_2, respectively, where S_1 and S_2 are boundary segments which together constitute the entire boundary of the region R. On S_1, the head is given while on S_2, the groundwater flux normal to the boundary is prescribed.

The region R in which the flow takes place is subdivided into a large number of discretized elements, in each of which the groundwater head is then approximated by a

simple function. Triangular or quadrangular elements are used because they make it possible to closely follow natural (curved) boundaries. This kind of subdivision also facilitates using a dense mesh in subregions of great interest and a coarse mesh in areas where the flow is of interest.

To approximate the variation of the head within an element the assumption was made that the head varies linearly within each element. The piezometric surface is thus approximated by a diamond-shaped surface, such that in each element the head is represented by a planar surface. The surface generated by such small planar elements, defined by the value at the nodal point, is a continuous surface, but slopes are discontinuous along the boundaries. The groundwater head at a point inside an element is defined by a linear interpolation between the value at the mesh points, (i.e. the nodes).

Therefore, piezometric head ϕ throughout the entire region can be expressed by:

$$\phi = \sum_{i=1}^{n} N_i(x, y) \, \Phi_i \tag{44}$$

where ϕ_i is the head at node i, and N_i is a shape

function or base function defined by :

$N_j = 1$, for $j = i$, $N_j = 0$, for $j <> i$

with linear interpolation within each element.

The problem is solved by a stepwise integration in time. The values at the end of a first time step is obtained, starting from the initial values. A next time step is then made by considering the values at the end of the first time step as the initial values for the second time step, etc.

A simple way to derive the basic algebraic equations of the numerical method is to integrate the differential equation (43) for t = 0 to t = Δt.   This results in:

$$\frac{\partial}{\partial x}(T\frac{\partial \phi}{\partial x}) + \frac{\partial}{\partial y}(T\frac{\partial \phi}{\partial y}) = s\frac{\partial \phi}{\partial t} - I \qquad \textbf{(45)}$$

where ϕ' is the value of the head at the end of the time interval considered, while the values of ϕ and I are averages over the time interval.   They are obtained by integration over Δt.

It is now assumed that the average value of the head ϕ during the time interval can be expressed in terms of the values at its beginning and its end in the form:

$$\phi = \epsilon \phi^0 + (1-\epsilon) \phi' \tag{46}$$

where ϵ is an interpolation constant, with $0 \leq \epsilon \leq 1$.

Formula (45) states that the average value is a linear combination of initial value and the final one, with different weights. For $\epsilon = 0$, the average value is equal to the final value. For $\epsilon = 1$, the average is equal to the initial value. In many practical cases, the transient processes are of a slowly decaying nature. This suggests that the average value should be slightly biased towards the final value with ϵ being somewhat smaller than 0.5. The value of ϵ will be an input parameter of the computer program.

By substituting Eq (46) into Eq (45), equation (45) becomes:

$$\frac{\partial}{\partial x}(T\frac{\partial \phi}{\partial x}) + \frac{\partial}{\partial y}(T\frac{\partial \phi}{\partial y}) + I - S\frac{\phi - \phi^0}{\Delta t (1-\epsilon)} = 0 \tag{47}$$

The time derivative has been eliminated by the process of integrating over the time step. As a result, an equation in

terms of the average value ϕ has been obtained.

In general, the approximation will not exactly satisfy the partial differential equation (46). Therefore, this condition is relaxed by requiring that the differential equation be satisfied only on the average, using a number of weighting functions equal to the number of unknowns. This is called the method of weighted residuals (Zienkiewicz, 1977). For more convenience, the shape functions N_i are used as weighting functions. This leads to the conditions:

$$\int_R \left\{ [\frac{\partial}{\partial x}(T\frac{\partial \phi}{\partial x}) + \frac{\partial}{\partial y}(T\frac{\partial \phi}{\partial y}) + I - S\frac{\phi - \phi^0}{\Delta t(1+\epsilon)}] N_i \right\} dxdy \qquad (48)$$

where $i \in C$ to be satisfied for each value of i for which ϕ_i is unknown. These values of i constitute a certain class, denoted by C.

C is the class of node numbers in which the value of the head is unknown. The values of i for all points of the boundary segment S_1 are excluded. Transmissivity T is assumed to be constant over the entire domain.

Satisfaction of Eq.(48) for all $i \in C$ will lead to just as many equations as there are unknown values (Bear and Verruijit, 1987).

Equation (48) can be separated into three integrals J_1, J_2 and J_3

$$J_1 + J_2 + J_3 = 0 \qquad (49)$$

for all $i \in C$

$$J_1 = \int_R \left\{ \frac{\partial}{\partial x} [N_i T \frac{\partial \phi}{\partial x}] + \frac{\partial}{\partial y} [N_i T \frac{\partial \phi}{\partial y}] \right\} dxdy \qquad (50)$$

$$J_2 = \int_R \left\{ T \sum_j \phi_j [\frac{\partial N_i}{\partial x} \frac{\partial N_j}{\partial x} + \frac{\partial N_i}{\partial y} \frac{\partial N_j}{\partial y}] \right\} dxdy \qquad (51)$$

$$J_3 = \int_R \left\{ I N_i - \frac{S}{\Delta t (1-\epsilon)} \sum_j N_i N_j (\phi_j - \phi_j') \right\} dxdy \qquad (52)$$

The summation in the second and third integrals should be

performed over all values of j from j = 1 to j = n, where n is the number of nodes. Equation (48) is the basic equation of the method of finite elements. Each of the three integrals will be evaluated separately.

The first integral J_1, as expressed by Eq (50), can be transformed into a line integral along the boundary S of the region R by the so-called divergence theorem or Gauss' theorem. This gives:

$$J_1 = \int_s \left\{ N_i T \frac{\partial \phi}{\partial n} \right\} ds \qquad (53)$$

where i ∈ C.

Thus, in the integration of the right hand side, the values of i are restricted to points located on the boundary S_2. The corresponding shape functions N_i are zero on S_1 and therefore, only a contribution from the integral along S_2 remains. On that part of the boundary, the value of $T(\partial \phi / \partial n)$ is known because it represents the amount of water Q_i supplied to the system at node i.

The second integral J_2 defined by Eq.(51) can be written formally as :

$$J_2 = -\sum_j P_{ij} \phi_j \qquad (54)$$

where the summation in the right-hand side means summation over all elements R_p included in the R domain and where:

$$P_{ij} = \int_{R_p} \left\{ T \left[\frac{\partial N_i}{\partial x} \frac{\partial N_j}{\partial x} + \frac{\partial N_i}{\partial y} \frac{\partial N_j}{\partial y} \right] \right\} dxdy \qquad (55)$$

To evaluate this integral, we first note that contributions to this integral can be expected only if element R_p contains both nodes i and j. If either node i or j do not belong to the integral, one of the shape functions is zero and, thus no contribution to the integral is made. Thus restriction can be made to elements containing both nodes i and j.

The shape functions are assumed to be linear in order to facilitate evaluation of this integral. The mathematical procedure is referred to (Reddy, 1984) and to (Bear and Verruijt, 1987).

The third integral J_3, defined by Eq.(52), may be regarded as consisting of two parts. The first part is an integral of the infiltration function I.

$$J_3-1 = \int \{IN_i\} dxdy \tag{56}$$

where i ∈ C.

For any particular value of i, the shape function N_i is different from zero only in the surrounding elements. If in all of these elements the infiltration function is assumed to be constant, which is only a minor restriction if the elements are sufficiently small, the integral over an element R_p actually expresses the average of the product $I_p N_i$ over that element, multiplied by the area of element.

The second part of the third integral can be written as:

$$J_{3-2} = -\sum_j \frac{S}{\Delta(1-\epsilon)} (\phi-\phi') \int_{R_p} \{N_i N_j\} dxdy \tag{57}$$

where i ∈ C.

Again, it is assumed that the physical parameters are constant. A complete mathematical development of the different integrals presented here is done by Bear and Verruijit, 1987.

It may be concluded that the solution of a nonsteady flow in an aquifer can be based on:

$$\sum_j [P'_{ij}\phi_j + R_{ij}(\phi_j - \phi_j^0)] = I_i \qquad (58)$$

where the coefficients P_{ij} and R_{ij} are obtained when solving numerically each of the three integrals J_1, J_2, j_3.

In order to improve the convergence when solving for Eq.(53) we used the Gauss-Seidel method. Practical experience with this method has shown that convergence can be improved by multiplying the correction in each updating step by a factor somewhat greater than 1. This means that in each step the error is not made equal to zero; it is made to change sign, in anticipation of future corrections.

Triangular elements lead to a certain asymmetry in most networks, because of the diagonal in a system of squares. This can be avoided by adding a second diagonal and an additional node in the center. However, this leads to almost

twice the number of nodes and elements in the mesh. It is more effective to compose a quadrangular element by considering it to be the sum of four triangular ones. Thus we will have only half as many elements, each with four nodes instead of three. As a consequence, the matrix must be generated in four steps for each of the composing triangles. Because a quadrangular element is considered the sum of two sets of two triangles, the effective transmissivity is doubled in the process. In order to account for this effect all transmissivity values should be reduced by a factor of 2.

A network of quadrangular elements may appear to be less flexible than a system of triangles because it seems to be less amenable to local refinements.

The same approach is used when modeling salty water intrusion. The governing differential equation is similar to Eq. (47), which describes groundwater flow. It can be written as :

$$\frac{\partial}{\partial x}(D_{xx}\frac{\partial c}{\partial x}) + \frac{\partial}{\partial y}(D_{yy}\frac{\partial c}{\partial y}) - v\frac{\partial c}{\partial x} - \frac{c-c_0}{(1-\epsilon)\Delta t} = 0 \qquad (59)$$

where v is an average velocity of the groundwater flow and D is the component of the dispersion tensor on both x and y directions. The same finite element mesh of triangular

elements, and linear interpolation functions are used in this advection-dispersion problem. The basic idea here is that the physical variables (the piezometric head, ϕ and the pollutant concentration, c) are defined at the nodes of a network of triangles, and that the linear interpolation in the element is performed by the definition of shape functions N_i (x,y).

The groundwater head, ϕ and the concentration, c are expressed as:

$$\phi(x,y) = \Sigma N_I(x,y)\phi_i \qquad (60)$$

$$c(x,y) = \Sigma N_i(x,y)c_i \qquad (61)$$

This means that the velocity, which is defined by the derivative of the head, is constant throughout each element.

Assuming that density and viscosity are not affected by changes in the concentration, the velocity distribution can be solved as a separate problem, independent of the solution of the concentration. We assume that the groundwater flow

problem has been solved, and that the velocity components in all direction can be considered as known.

The finite element equation is then derived in a flow model with a Galerkin approach. This means that the partial differential equation (56) is multiplied by each of the shape functions, and that the result is integrated over the domain. Each of the surface integrals is evaluated by a summation of integrals over triangular elements. By an appropriate rotation of the coordinate system in an element, the X-axis can always be made to coincide with the direction of the flow, so that for the evaluation of the integral over a single element can always be written in the form of Eq.(56).

IV. RESULTS AND DISCUSSIONS

Estimated values of hydraulic conductivity obtained by applying the Lefranc test are presented in table (4) and figure (9). These values are also compared with those obtained using the Slug test for several piezometers where both methods have been performed with success.

A general conclusion on both techniques, which have been previously described in chapter III, is also drawn.

The analysis of the spatial variability of the hydraulic conductivity is performed using a geostatistical package (Geostat 1986), based on universal kriging and developed by ORSTOM.

1. LeFranc Test Results.

This test has been applied with success in approximately 72 piezometers. Field data collected during the test are presented in Appendix A. Estimation of local hydraulic conductivity values are made using Maurice Cassandre's resolution in "les essais d eau dans la reconnaissance des sols", (Eq (21) thru Eq (36)).

The computed values of hydraulic conductivity are relatively small, mostly in the range between 10^{-4} and 10^{-6} cm/sec. The smallest values were found in locations where a relatively high level of salinity was present.

88
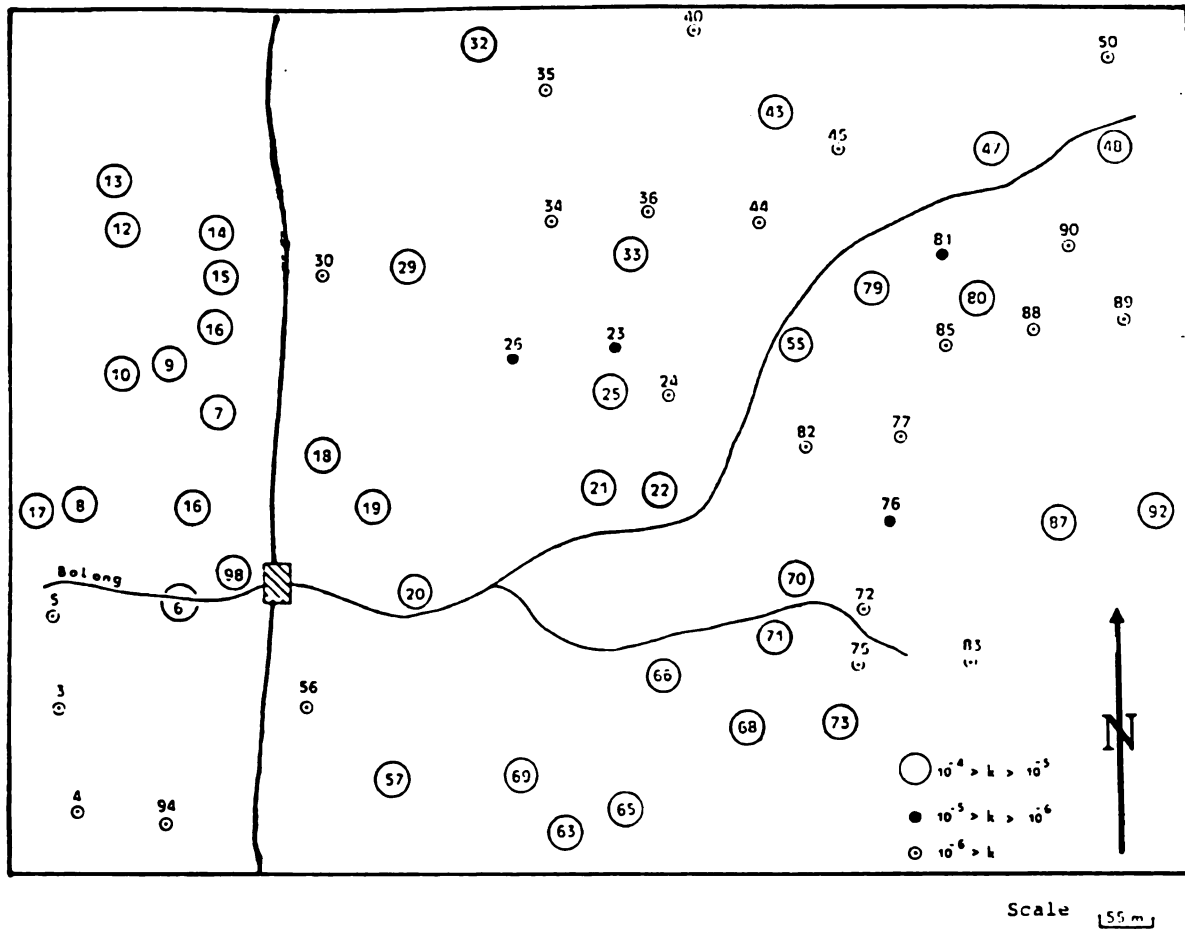
Figure 9.   Spatial distribution of hydraulic conductivity.

Table 4. Estimated values of hydraulic conductivity by LeFranc test. K .10^{-6} (cm/sec)

Pi	K	Pi	K	Pi	K	Pi	K	Pi	K
3	74	19	180	35	77	63	330	83	20
4	51	20	190	36	18	65	400	85	25
5	2.5	21	190	39	100	66	350	87	190
6	280	22	250	40	36	68	260	88	61
7	280	23	5.6	43	130	70	600	89	95
8	500	24	94	44	96	71	190	90	34
9	290	25	180	45	60	72	24	92	220
10	320	26	7.3	47	240	73	160	93	310
12	150	27	150	48	240	75	91	94	17
13	210	28	8	50	35	76	5.7	97	230
14	330	29	210	55	380	77	60	98	260
15	230	30	52	56	80	79	380	−	−
16	190	32	760	57	390	80	150	−	−
17	170	33	200	61	76	81	8.9	−	−
18	170	34	67	62	140	82	92	−	−

2. Slug Test Results.

This second technique was conducted in a few randomly selected piezometers. The principles are described in chapter III. The field data collected are then analyzed using a set of equations (Eq 37 thru Eq 40), and the results are presented in table (5).

Most of the data collected at many piezometers cannot be interpreted because of a relatively small drawdown. The curve obtained using a log-log scale is simply a horizontal line that cannot be superimposed on any of the characteristic used when applying the Slug Test.

Table 5. Slug test results K 10^{-6} (cm/sec)

Piezometer Number	Hydr.cond K (cm./s)	Piezometer	Hydr.cond K (cm./s)
23	5.6	71	190
36	20	77	35
49	220	83	20
56	71	88	65
63	290	92	180

3. Comparison between LeFranc Test and Slug Test.

Results obtained by both techniques at the piezometers are quite similar. The differences between the values of hydraulic conductivity are relatively small or even negligible. This confirms the validity of the results obtained by each of the two techniques, especially by the LeFranc test, which has been conducted with success on more than three quarters of the installed piezometers.

The fact that most of the field data collected during the Slug test cannot be analyzed seems to indicate that this technique is less effective.

Table 6. Comparison between LeFranc test and Slug test K 10^{-6} (cm/sec.)

Piez	LeFranc	Slug	Piez	LeFranc	Slug
23	5.6	5.6	77	60	35
36	18	20	83	20	20
56	80	71	88	61	65
63	330	290	92	220	180
71	190	190	–	–	–

The spatial distribution of the hydraulic conductivity shows that the highest values of hydraulic conductivity are located in two zones within the study area (Fig 9). Indeed, these regions correspond to the main entrance of salt water into the drain and to the South-western part of the valley around piezometer 73.

Geostatistical analysis of the hydraulic conductivity shows that the distribution is partially random. The estimated or experimental variogram of the field data (Fig. 10) is compared with a spheric model. Output of the program is presented in Appendix A. The most important information we can obtain from (Fig. 10) is the path of the variogram, or the best sampling distance. As it can be shown in (Fig. 10), the best sampling distance is about 80 meters. This means that approximately half of the measurements would be enough to obtain a good estimation and representation of the spatial variability of the studied parameter.

The sampling distance resulting from the universal kriging will be used later in order to define an appropriate mesh for ground water flow modelling using the Finite Element method.

The parameters required for modelling the experimental variogram in this case-study are the drift coefficient, which is estimated at 0.6, the number of neighboring points (10

points), and the sampling distance (80 meters). The experiment then consisted of kriging each observation using neighboring points and using various measures between krigged values and known values as criteria for assessing the validity of the assumed underlying drift and covariogram models.

4. Estimation of Groundwater Flow.

Graphical techniques are used to evaluate groundwater flow in the study area. This method is based on an interpretation of a contour map representing piezometric heads and water salinity at several points in time (Fig. 11, 12, 13, 14, 15). The contour maps are obtained using a Golden Software package (SURFER Version 4.1), which is based among other techniques in Universal Kriging.

A Study of three contour maps representing piezometric heads in February, April and, June (Fig. 11, 12, 13), shows that there is no predominant flow direction for the groundwater. On the contrary, water flows in all directions. One of the main reasons is that the region is quite flat with many depressions which can be seen as major evaporative zones acting like convergency points for groundwater flows. Contour maps of groundwater salinity are presented in (Fig 14, 15).

Superimposing both kinds of contour maps, it appears clearly that in February and in April salt water flows from
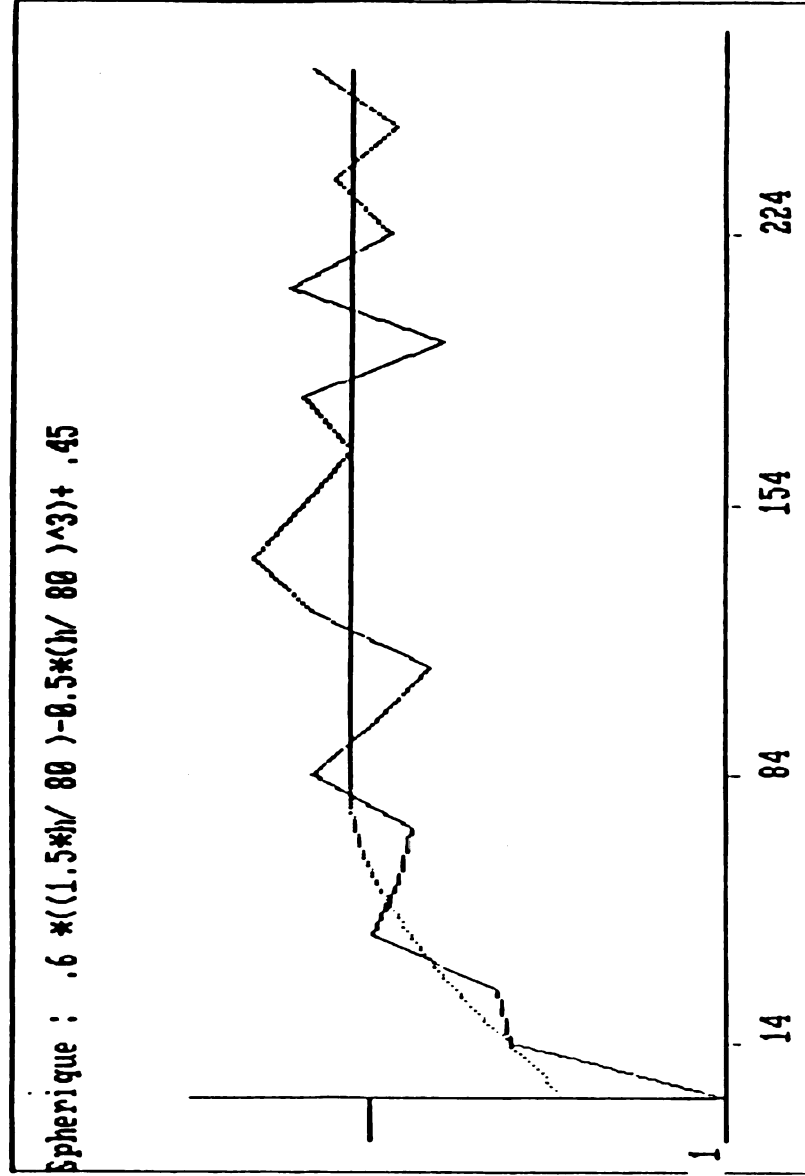
Figure 10. Variogram of hydraulic conductivity values.

the river *(Bolong)* towards the North and pours out into a drainage axis, which can be defined by a line connecting piezometers 15, 30, and 23.

Fresh water (electrical conductivity < 1 mS) from the piezometric dome in the northern part of the valley flows towards the same drainage axis. As a result, we observe a partial dilution of the salt water which then flows towards the south-east, and the east into a large depression that also collects flows coming from the terraces located at the northern and eastern parts of the study area (Fig. 11, 12, 13).

This depression is certainly an evaporative area that provokes a fast increase of salinity during the dry season.

Based on Fig (12), flow rates for both salt and fresh water converging towards the large depression located at the north-western part of the study area are computed as follows.

4.1. Fresh water flow rate.

Estimation of fresh water flow rate is based on Darcy's law, Eq (1) (Q = K Si).

Where: K = Field average of hydraulic conductivity: 2.5 10^{-6} m/sec.

b = Aquifer thickness: 33 meters (B. Dieng et Le Priol. 1986).

L = Average distance between equipotential lines from the contour map of the observed piezometric heads 04/14/87 L : 130 meters.

S = Flow crossection: 302 * 33 = 10^4. m^2.

i = Hydraulic gradient: dh/L = 0.25/130 =$1.9.10^3$.

Q = 2.5 10^{-6} m/sec. * 10^4 m^2 * 1.9 10^{-3} = 4.7 10^{-5} m^3/sec.

4.2. Salt water flow rate.

Estimation of salt water flow rate is much more difficult because, theoretically, Darcy's law cannot be applied when water salinity reaches a high level. One way of solving this problem is to compute the equivalent fresh water for those piezometers where high concentration of salt, mainly NaCl, is present.

Based on the fact that values of hydraulic conductivity are very small and that, for most parts of the valley, groundwater is contaminated with salt intrusion with various levels of concentration, we assume for the purpose of flow rate estimation that Darcy's law holds. This assumption is indeed a simplification of a very difficult problem.

S = 319 * 33 = 10.5 m^2

i = 0.25/271.3 = 9.2 10^{-4}

Q = 2.5 10^{-6} m/sec. * 10.5 m^2 * 9.2 10^{-4} = 2.4 10^{-5} m^3/sec.

Fresh water flow rate is higher than that of salt water. Electrical conductivity values in the drainage axis are intermediate between those of fresh and salt water; this confirms a certain dilution of salt water.

In June, groundwater flow remains almost the same regardless of the amount of precipitation at the beginning of the rainy season.

The depression observed in February and April still exists in June and receives water from all directions.

5. Groundwater flow model.

Based on estimation of hydraulic conductivity over the entire study area, an attempt to model groundwater flow using a numerical procedure is made. Finite element techniques are used to solve the basic flow equation (Eq (13)). The computer program is written in Quick Basic version 4.5. It is derived from a set of examples developed and presented by Bear and Verruijit, 1987. A listing of the computer program is presented in Appendix B.

The finite element mesh is presented in Fig.(16). Several assumptions have been made, among them the Dupuit assumption (cf. Chapter III). All elements are rectangular and have approximately the same size. The total number of rectangular elements is 109. The aquifer is considered to be
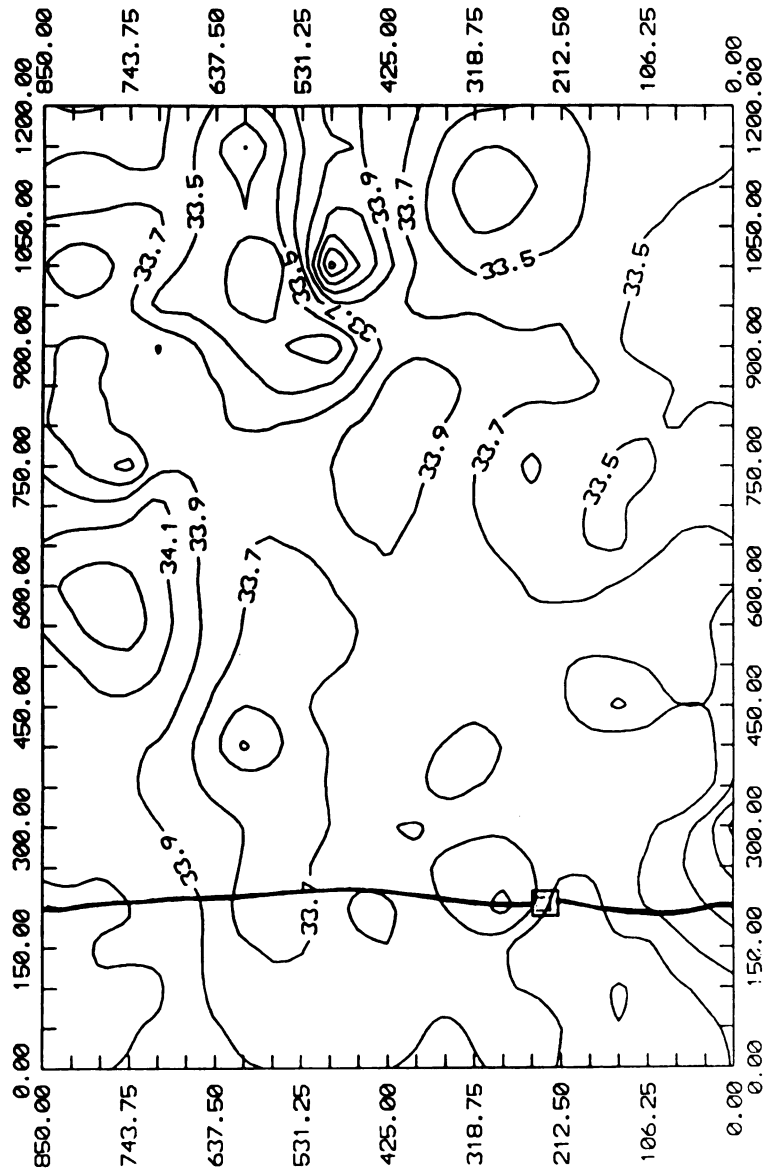
Figure 11. Observed piezometric heads 02/03/87
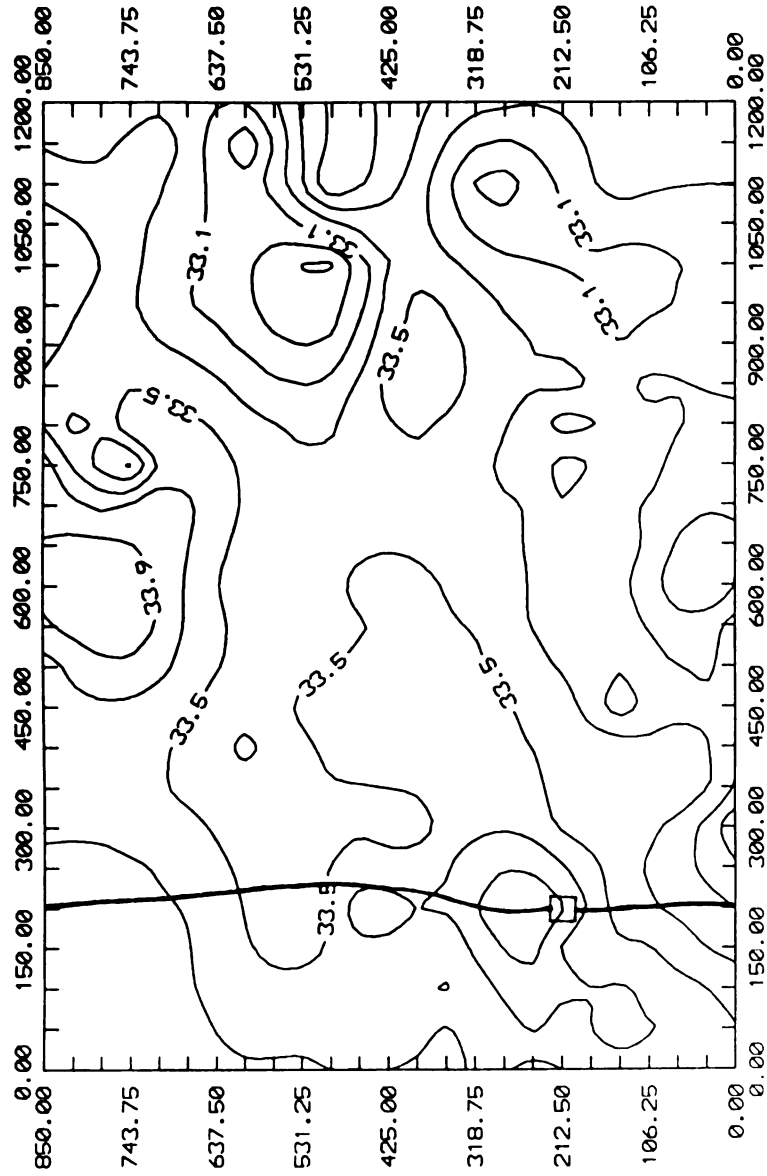
Figure 12. Observed piezometric heads 04/14/87.
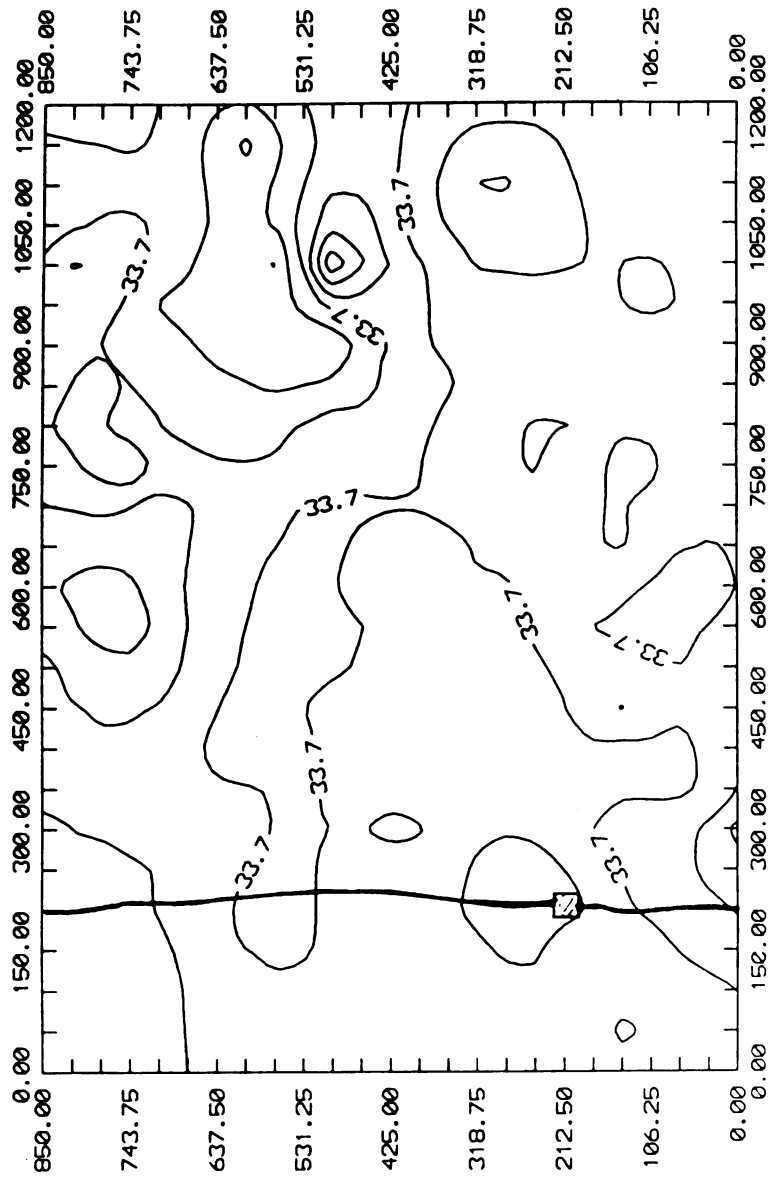
Figure 13.   Observed piezometric heads 06/30/87.
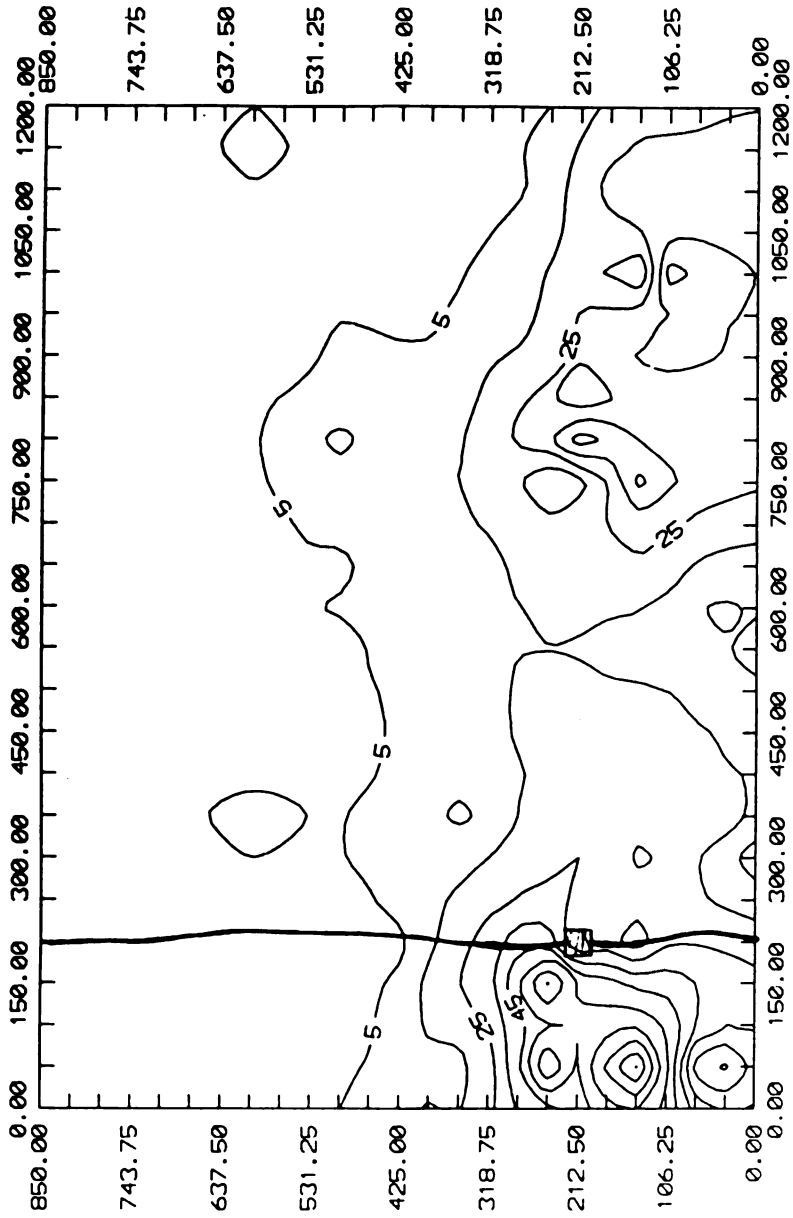
Figure 14. Groundwater salinity 02/03/87.
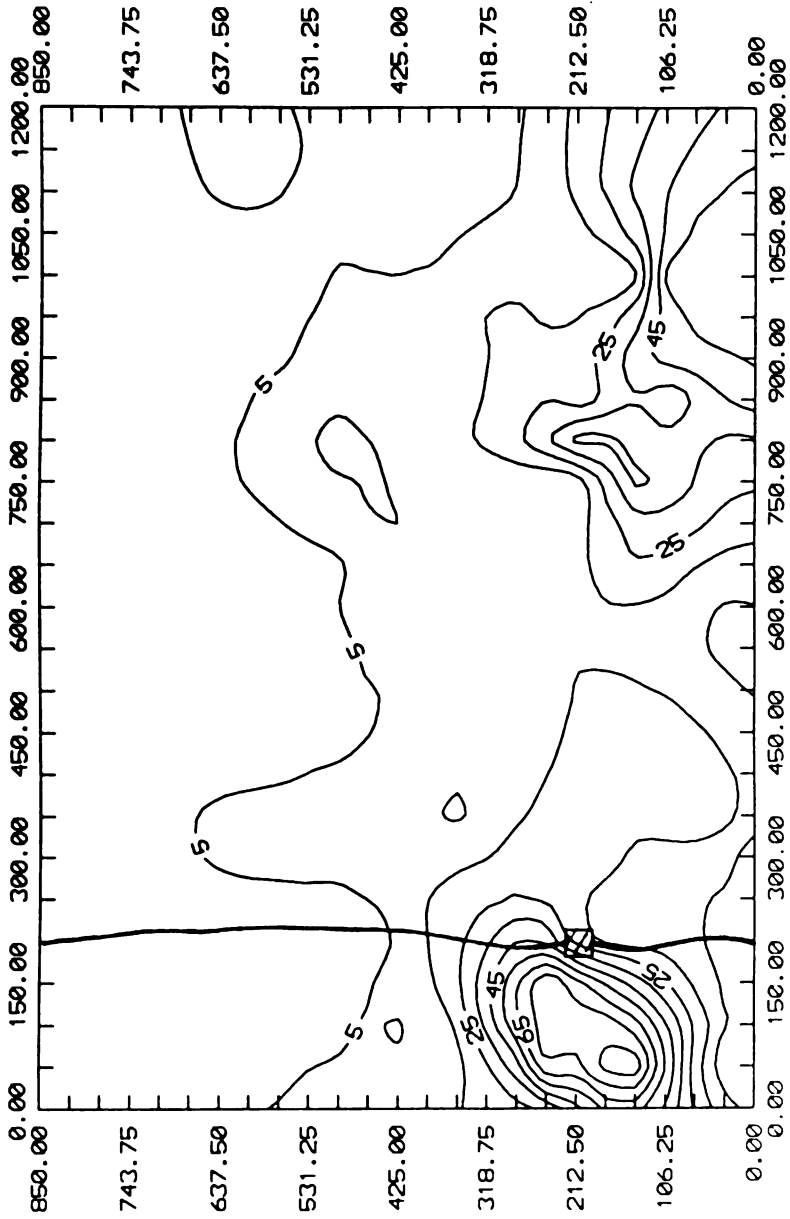
Figure 15. Groundwater salinity 06/30/87.
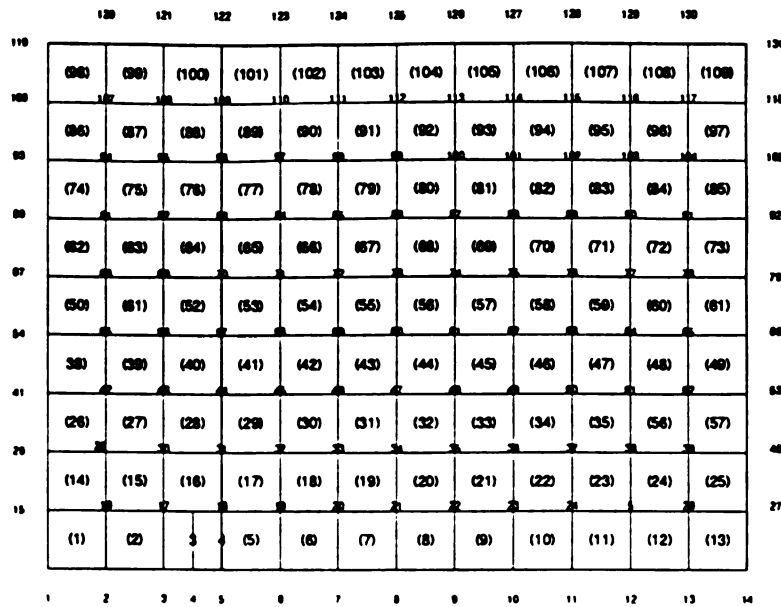
Figure 16.   Finite element mesh for Katoure Valley.

infinite, homogeneous and intrinsic with a constant thickness (33 meters) and has a field average hydraulic conductivity of $2.5\ 10^{-6}$

5.1. Model Description.

The program uses interactive input, with self-explanatory input prompts. The program asks first for some geometrical data which define the mesh. Then it asks for physical parameters: the initial head, the infiltration rate, the transmissivity and the storativity. If the head at node (I) is given then the type-indicator IP (I) is set equal to 1; if not, the value of IP (I) is set equal to -1. The program then asks for the rate of local water supply.

All these parameters are considered constant throughout the region. The program asks then for a value for the time step.

The actual calculations are performed in lines 4055-5400 as follows:

5.1.1. Genetation of Systems Matrix

When all the input data have been entered, the system matrix {P} can be generated. This is performed in lines 3220-4040. For a particular element as indicated by the variable J, the coordinates of the nodes are stored in the variable XJ(I) and YJ(I). Then the coefficients B(I) and C(I)

and the determinant D are calculated based on the mathematical development of Eq (52). This then enables us to calculate the values of the matrix {P} for element J and stores them in the appropriate positions of the matrix, as defined by KK and LL. Note that the summation over all elements is performed by adding the contributions from each element consecutively to the matrix {P}, which is initially filled with zeros.

5.1.2. Solution of Equations.

The system of equations is solved by the Conjugate Gradient Method, in lines 4050 -5400. This method is usually effective when it comes to computer memory requirement and time of computation. It also allows the use of a pointer matrix; it is very simple to account for the boundary conditions without the need to modify the system matrix. After completion of NI iterations, the values of F(I) are calculated and the solution is finally printed.

As in all transient solutions, the magnitude of the time steps deserves some special attention. Because the finite element method is very similar to the finite difference method, it can be expected that for a value of ε in the range from $\varepsilon = 1/2$ through $\varepsilon = 1$, the numerical process is unconditionally stable. This is indeed observed when the program is executed. Also, to obtain sufficient accuracy, it is suggested that the first time step be of the order of

magnitude:

$$\Delta t = \frac{S(\Delta x)^2}{2T} \qquad \qquad (62)$$

where Δx denotes a characteristic measure for the mesh and T the transmissivity. Because in the present case study the mesh size is 100 meters and the transmissivity T = 0.25 m/day, it follows that the first time step should be 8000 days.

5.2. Model Validation.

The developed numerical model was tested on an example from Segerlind (1984). The simulated piezometric heads are presented in Appendix A, together with the actual heads reported by Segerlind (1984). Figure (17) shows a good correlation between the two series of data. This demonstrates that the developed numerical model is working realistically.

For this study three scenarios were tested. They represent pressure heads in February, April and, June. For all scenarios it is assumed that there is only one given pressure head at node (5) and an average field flow rate for

all elements. Node (5) is monitored well, located outside the paddy fields on the side of the valley. In February, the average flow rate is 4 $10^{-5} m^3$/sec. and the given head is 34 meters; in April, the average flow rate is assumed to be 3 $10^{-5} m^3$/sec. and the given head 33.50 meters. In June, the flow rate is 2.50 10^{-5} m^3/sec. and the given head 32.50 meters. Unlike the two previous months, it is assumed that at time $t= 0$, uniform infiltration starts on the entire area of the aquifer at a constant rate of I = 0.005 m/day.

After performing the finite element calculations, the predicted values of pressure heads along the free surface were compared with the observed values at the same node points and for the same time period. Simple linear regression using Statgraphics version 2.6 is used for all three scenarios in order to test for the model validation. We assumed that both observed and predicted pressure heads are random variables. Results of the test are presented in Appendix C. They show that there is a good correlation between the observed and the predicted head pressures for the first two scenarios (R^2, respectively 0.89 and 0.99). For the third scenario, the test shows that there is almost no correlation between observed and predicted variables $R^2 = 0.12$. Reasons for this can be found in the set of assumptions made earlier. The assumption that the groundwater is fresh everywhere in the area and that
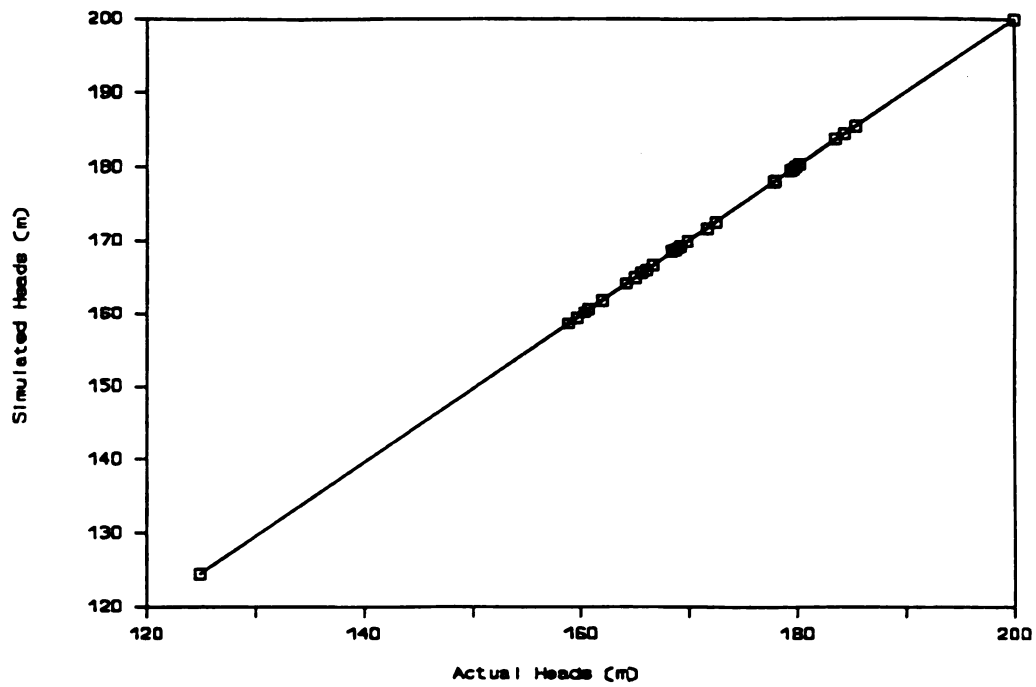
Figure 17. Model validation.

infiltration is also at a constant rate all over the finite element mesh cannot hold. The study area should be divided into homogeneous subregions based on soil type and hydraulic conductivity of the unsaturated zone. Because of the long dry season that ends in May, the groundwater salinity is extremely high in June, and that particular attention should be given to establishing the equivalent fresh water head pressure.

6. Discussion.

This present case study shows that among the field techniques used, the LeFranc test is the most reliable. This technique is easy to replicate and the results give a good estimation of the hydraulic conductivity. However, in a situation like Katoure valley where we do have a salt water intrusion and a dilution problem, a more cautious attitude should be taken when interpreting the results. This can be done by applying other field techniques on randomly selected points and comparing the different results. Because of the spatial variability of soil's physical parameters, a geostatistical analysis is highly necessary.

The small values of hydraulic conductivity and tansmissivity indicate that groundwater flow in this case study is under the influence of vertical fluxes, like evaporation or infiltration. Indeed, the drawdown
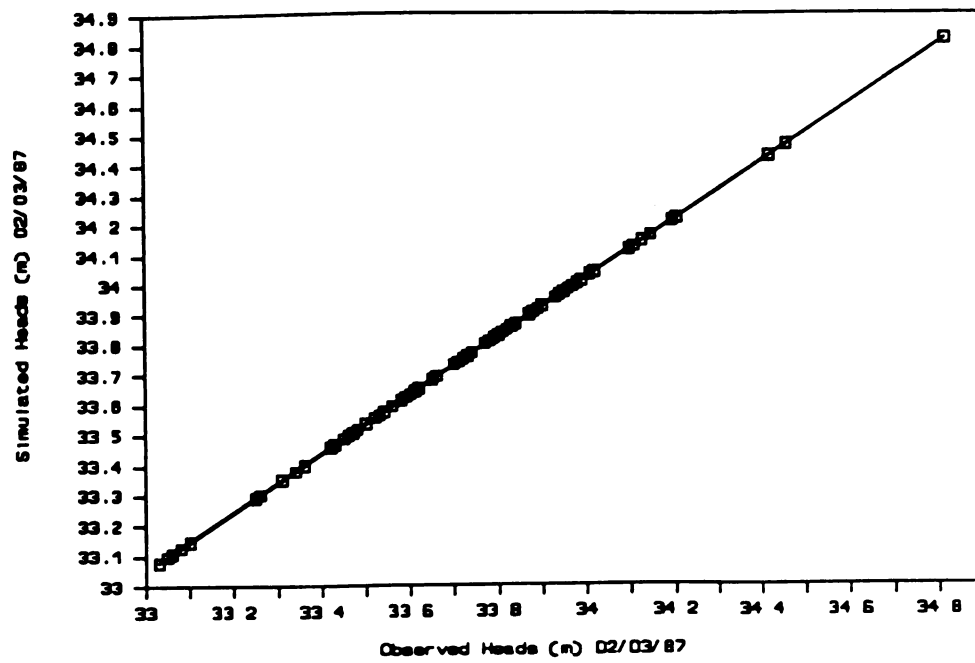
Figure 18. Plot of simulated versus observed heads 02/03/87.
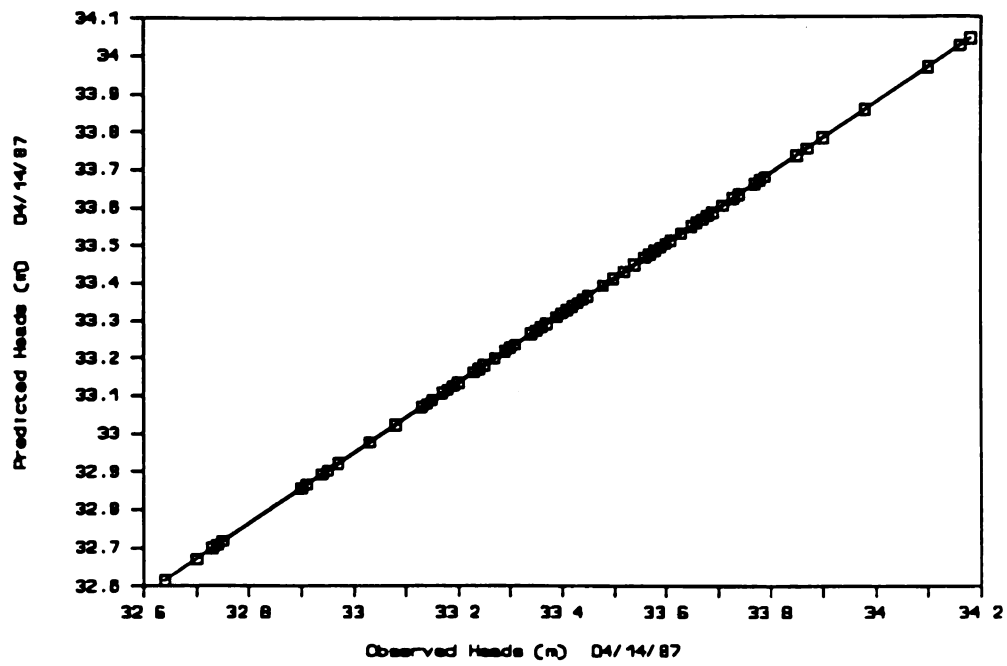
Figure 19. Plot of simulated versus observed heads 04/14/87.
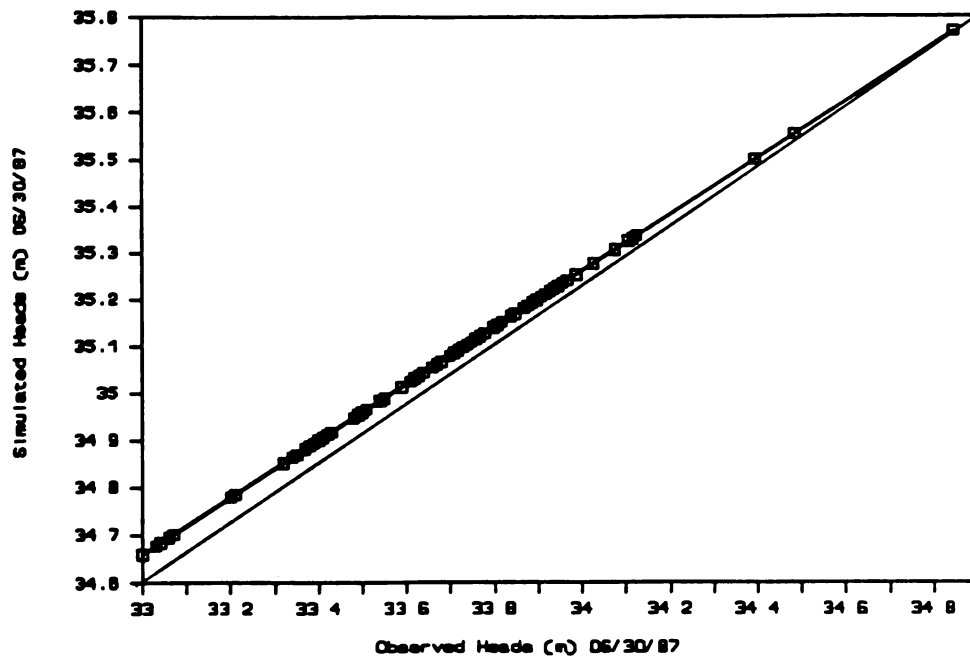
Figure 20. Plot of simulated versus observed heads 06/30/87.

during the dry season is very important and the amount of precipitation at the beginning of the rainy season in June raises the watertable level very fast. It can be said, however, that flow rates of fresh or salty water are quite small and groundwater flows in all directions towards some large depressions. These depressions can be considered as high potential evaporative zones where, during the dry season, intermediate values of electrical conductivity due to the mixing of both fresh and saline water are observed.

Contour maps of groundwater salinity show that, during the dry season, salt water intrusion from the river (*Bolong*) is very important and represents a real problem for farmers growing vegetables in the side of the valley. Because use of fresh water in the side of the valley is very intensive, salt water reaches most of these gardens very quickly.

The simulation program presented in this thesis can be used as a prediction tool for future behaviors of groundwater flow. However, particular attention has to be given to the fact that we do not have a homogeneous medium, at least from a water salinity point of view. The finite element mesh must include as one of its criteria for homogeneous elements, soil type and infiltration rates for the unsaturated zone. These parameters are very important if we want to better predict future behavior of the groundwater during the rainy season and

after specific storms.

The numerical model developed can be used for evaluating water management policies, mainly during the dry season. Plots of the observed as well as the simulated data (Appendix C) show that salt water intrusion happens most of the time during that period of the year. By intensively pumping the groundwater to irrigate the increasing area under vegetable growing every year, farmers create a very important drawdown that provokes salt water intrusion. As a consequence most of the gardens on the terraces are abandoned after only one year of exploitation. Using this numerical model one can estimate how much water (pumping rate) should be pumped to maintain a balance that will reduce the magnitude of the salt intrusion and secure at least a vegetable production.

This model can also provide interesting information when planning for future water use. Simulated piezometric heads together with contour maps of water quality are an important criterion in the selection of agricultural field locations with saline water tables close to the surface and where artificial subsurface drainage should be installed.

V. CONCLUSIONS AND RECOMMENDATIONS

A study of groundwater flow and quality in an ancient mangrove plain like Katoure valley was made difficult by the complexity of encountered problems due basically to soil heterogeneity and presence of salt water. Field techniques for estimating soil and water parameters, as well as methods of analyzing collected data, have to be cautiously selected. Because of the spatial variability of soil's physical parameters, a geostatistical analysis is necessary. Often, this leads to making assumptions that can sometimes introduce significant errors.

The finite element method proved to be an excellent tool for simulating groundwater flow and quality in such complex media. This method is particularly flexible when dealing with irregular boundaries as well as important heterogeneity problems. This is indeed the main problem one has to solve when studying groundwater in a mangrove ecosystem like the Lower Casamance region of Senegal.

Today, the primary issues of concern relating to future impacts of anti-salt dams are:

1. groundwater levels,

2. groundwater contamination by sea water intrusion,

3. soil salinization as a result of salt water intrusion and high evaporation potential,

4. flatness of the terrain which makes natural drainage almost impossible in many locations.

The proposed numerical model developed as part of this study already addresses most of these concerns. However, to better estimate the real impact of the Katoure anti-salt dam, this model has to be coupled with one which would predict groundwater quality. Therefore, by combining both models, real perspectives for a good management decisions could be made. This will be the key factor for the success of the anti-salt dams policy. Today sufficient data on the Lower Casamance region are available.

APPENDICES

Model Validation

Table A-1: Actual head values by Segerlind (1984) and simulated head values using the developed numerical model.

Nodes	x (m)	y (m)	Actual H (m)	Simulated H (m)
1	0.00	0.00	200.00	200.00
2	0.00	1000.00	200.00	200.00
3	0.00	2000.00	200.00	200.00
4	0.00	3000.00	200.00	200.00
5	1000.00	0.00	180.20	180.09
6	1000.00	500.00	179.60	180.40
7	1000.00	1000.00	178.00	177.60
8	1000.00	2000.00	177.90	177.80
9	1000.00	2500.00	179.40	179.40
10	1000.00	3000.00	179.80	180.10
11	1500.00	1000.00	166.10	165.40
12	1500.00	1500.00	164.30	163.80
13	1500.00	2000.00	165.70	166.10
14	2000.00	0.00	169.00	168.50
15	2000.00	500.00	166.70	166.30
16	2000.00	1000.00	160.40	158.50
17	2000.00	1500.00	124.90	125.60
18	2000.00	2000.00	159.70	157.5019
19	2000.00	2500.00	165.10	165.00
20	2000.00	3000.00	169.30	167.80
21	2500.00	1000.00	162.00	162.10
22	2500.00	1500.00	158.90	157.80
23	2500.00	2000.00	160.80	160.60
24	3000.00	0.00	172.50	172.40
25	3000.00	500.00	171.70	171.30
26	3000.00	1000.00	169.90	169.50
27	3000.00	2000.00	168.30	168.50
28	3000.00	2500.00	168.70	168.80
29	3000.00	3000.00	168.70	168.70
30	4000.00	0.00	185.50	185.30
31	4000.00	1000.00	184.30	184.30
32	4000.00	1500.00	183.50	183.50
33	4000.00	2500.00	179.50	179.40
34	5000.00	0.00	200.00	200.00
35	5000.00	1000.00	200.00	200.00
36	5000.00	2000.00	200.00	200.00

Table A-2: Pressure heads simulation results

Node #	Coordinates (meters)		Pressure Heads (meters)		
	X	Y	02/03	04/14	06/30
1	0	0	33.83	33.42	34.72
2	100	0	33.69	33.26	34.90
3	200	0	33.38	32.94	35.20
4	300	0	33.03	32.60	35.23
5	350	0			
6	400	0	33.52	33.01	35.12
7	500	0	33.55	33.02	34.74
8	600	0	33.69	33.38	34.29
9	700	0	33.60	33.36	34.19
10	800	0	33.57	33.23	34.12
11	900	0	33.42	33.12	34.04
12	1000	0	33.43	34.14	33.94
13	1100	0	33.52	33.24	33.90
14	1200	0	33.56	33.30	34.00
15	0	100	33.95	33.60	34.73
16	100	100	33.92	33.50	34.86
17	200	100	33.64	33.22	35.21
18	300	100	33.61	33.22	35.28
19	350	100	33.72	33.26	35.25
20	400	100	33.65	33.21	35.28
21	500	100	33.72	33.12	34.82
22	600	100	33.45	33.88	34.40
23	700	100	33.44	33.25	34.20
24	800	100	33.42	33.14	34.16
25	900	100	33.40	33.01	34.15
26	1000	100	33.53	33.00	34.03
27	1100	100	3.56	33.24	34.03
28	1200	100	33.53	33.31	34.00
29	0	200	33.55	33.45	34.74
30	100	200	33.84	33.66	34.87
31	200	200	33.82	33.86	34.54
32	300	200	34.12	33.40	33.88
33	400	200	33.82	33.26	34.68
34	500	200	33.76	34.16	33.61
35	600	200	33.65	33.17	33.52
36	700	200	33.59	33.19	34.32
37	800	200	33.49	33.84	34.62
38	900	200	33.40	33.17	34.25
39	1000	200	33.50	33.95	34.06
40	1100	200	33.36	33.02	33.89
41	1200	200	33.38	33.26	34.13
42	0	300	33.35	33.60	34.76
43	100	300	33.50	33.52	35.00
44	200	300	33.81	33.80	34.82
45	300	300	33.86	33.60	34.43
46	400	300	34.25	33.44	34.76

Table A-2 (continued)

Node #	Coordinates (meters)		Pressure Heads (meters)		
	X	Y	02/03	04/14	06/30
47	500	300	33.97	33.38	34.75
48	600	300	33.85	33.31	34.54
49	700	300	33.78	33.29	34.43
50	800	300	33.71	33.32	34.84
51	900	300	33.2	33.39	34.42
52	1000	300	33.46	33.10	34.07
53	1100	300	33.55	33.76	34.94
54	1200	300	33.37	33.32	33.38
55	0	400	33.07	33.67	34.90
56	100	400	33.51	34.44	33.85
57	200	400	33.88	33.58	33.85
58	300	400	33.80	33.40	34.40
59	400	400	33.60	33.52	35.05
60	500	400	33.68	33.49	35.04
61	600	400	33.85	33.44	34.87
62	700	400	33.82	33.37	34.75
63	800	400	33.80	33.47	34.60
64	900	400	33.70	33.50	34.10
65	1000	400	33.76	3.34	33.71
66	1100	400	33.73	33.29	34.94
67	1200	400	33.79	33.46	34.25
68	0	500	33.55	33.64	34.99
69	100	500	33.66	33.52	34.87
70	200	500	33.85	33.55	34.87
71	300	500	33.77	33.44	34.87
72	400	500	33.70	33.51	34.74
73	500	500	33.82	33.45	34.92
74	600	500	33.12	33.37	35.10
75	700	500	34.80	33.30	35.04
76	800	500	33.93	33.20	34.97
77	900	500	33.87	34.88	35.11
78	1000	500	33.90	33.26	34.24
79	1100	500	33.78	33.84	33.86
80	1200	500	33.60	33.70	35.17
81	0	600	33.74	33.77	35.05
82	100	600	33.44	33.55	35.14
83	200	600	33.66	33.51	35.19
84	300	600	33.70	33.41	34.11
85	400	600	33.80	33.20	34.84
86	500	600	33.55	33.41	35.13
87	600	600	33.23	33.40	3.28
88	700	600	33.40	33.40	35.26
89	800	600	33.30	33.30	35.14
90	900	600	33.30	33.01	34.67
91	1000	600	33.96	32.96	34.02
92	1100	600	34.80	32.94	34.19

Table A-2 (continued)

Nodes #	Coordinates (meters)		Pressure Heads (meters)		
	X	Y	02/03	04/14	06/30
93	1200	600	33.93	32.94	34.19
94	0	700	33.87	33.75	35.02
95	100	700	33.90	33.77	35.03
96	200	700	33.78	33.46	35.12
97	300	700	33.60	33.44	35.22
98	400	700	33.74	33.66	35.24
99	500	700	33.44	33.81	35.37
100	600	700	33.66	34.67	35.55
101	700	700	33.70	33.50	33.52
102	800	700	33.80	33.27	35.10
103	900	700	33.55	33.13	35.25
104	1000	700	33.23	33.18	34.18
105	1100	700	33.20	33.09	34.39
106	1200	700	33.24	33.75	34.35
107	0	800	33.37	33.71	35.06
108	100	800	34.05	33.62	35.10
109	200	800	34.13	33.52	35.19
110	300	800	33.98	33.49	35.23
111	400	800	33.90	33.61	35.23
112	500	800	33.87	33.96	35.25
113	600	800	34.11	33.53	35.35
114	700	800	34.18	33.13	35.80
115	800	800	34.07	33.38	35.40
116	900	800	33.71	33.46	34.97
117	1000	800	33.52	33.26	34.90
118	1100	800	33.57	33.00	34.42
119	1200	800	33.64	33.84	34.98
120	0	850	33.69	34.87	33.90
121	100	850	34.12	33.83	35.06
122	200	850	34.16	33.67	35.12
123	300	850	34.12	33.62	35.20
124	400	850	34.00	33.61	35.15
125	500	850	33.96	34.00	35.24
126	600	850	34.07	33.82	35.26
127	700	850	34.34	33.49	35.63
128	800	850	33.97	33.54	35.37
129	900	850	33.60	33.58	35.02
130	1000	850	33.74	33.42	34.86
131	1100	850	34.01	33.17	34.90
132	1200	850	33.50	33.19	34.93

Table A-3:   Observed pressure heads.

Piez. #	coordinates (meters)		Pressure Heads (meters)		
	X	Y	02/03	04/14	06/30
1	150	200	33.83	33.56	34.13
2	100	150	34.13	33.73	34.38
3	50	150	34.10	33.77	34.59
4	50	50	33.99	33.66	33.98
5	50	250	33.85	33.77	34.33
6	150	250	34.10	33.98	34.17
7	200	450	34.01	33.87	34.17
8	50	350	33.96	33.78	34.73
9	150	500	33.73	33.50	34.00
10	100	500	33.77	33.57	34.03
11	50	550	33.82	33.66	34.94
12	100	650	33.87	33.63	33.93
13	100	700	33.13	33.85	34.10
14	200	600	33.59	33.48	33.47
15	200	650	33.94	33.67	33.62
16	150	350	33.81	33.56	33.29
17	0	350	33.95	33.77	34.61
18	300	400	33.65	33.35	34.09
19	350	350	33.99	33.65	34.02
20	40	250	33.78	33.30	33.67
21	60	350	33.79	33.41	33.87
22	650	350	33.78	33.45	33.48
23	650	500	33.74	33.39	34.46
24	700	450	33.02	33.36	34.02
25	600	450	33.89	33.61	33.63
26	550	500	33.50	33.30	33.54
27	450	500	33.81	33.66	33.54
28	450	700	34.01	33.60	34.00
29	400	600	33.25	33.25	33.71
30	350	600	33.66	33.39	33.21
31	550	750	34.46	34.10	33.21
32	500	850	33.93	33.61	33.64
33	650	600	33.70	33.43	34.36
34	600	650	33.83	33.54	33.66
35	600	800	34.42	34.17	33.46
36	700	650	33.83	33.63	33.95
37	700	700	34.19	33.87	34.73
38	700	750	34.02	33.71	33.90
39	750	750	33.34	32.97	33.83
40	750	850	33.88	33.79	34.27
41	750	700	33.90	33.58	33.27
42	800	750	33.80	33.68	34.31
43	800	650	33.71	33.52	34.58
44	900	700	33.95	33.30	34.82
45	950	700	33.36	33.14	33.68

Table A-3 (continued)

Piez #	Coordinates (meters)		Pressure Heads (meters)		
46	1050	700	33.71	33.24	33.91
47	1150	700	33.72	33.43	34.03
48	1100	800	33.48	33.34	33.25
49	1200	800	33.95	33.08	32.90
50	1050	850	33.71	33.59	33.86
51	1000	800	33.15	33.58	33.62
52	900	800	33.62	33.45	34.08
53	800	800	33.59	33.15	33.22
54	800	500	33.84	33.27	33.63
55	300	150	33.74	33.39	33.64
56	300	150	33.94	34.39	33.42
57	350	50	33.84	33.44	33.62
58	400	150	33.42	33.43	33.14
59	450	150	33.70	33.95	33.45
60	450	200	33.61	33.40	33.53
61	450	100	33.80	33.19	33.65
62	500	50	33.53	33.34	33.28
63	550	0	33.88	33.23	33.78
64	550	150	33.97	33.18	33.80
65	600	50	33.43	33.77	33.30
66	650	150	33.47	33.13	33.64
67	750	150	33.66	33.20	33.37
68	750	200	33.43	33.43	33.51
69	750	250	33.61	33.18	33.88
70	800	250	33.46	33.23	33.55
71	800	200	33.90	32.91	33.91
72	850	200	33.56	33.41	34.00
73	850	100	33.42	33.36	33.63
74	900	100	33.52	33.17	33.62
75	900	150	33.56	33.08	33.91
76	800	500	33.86	33.20	33.89
77	950	300	33.10	33.31	32.90
79	950	400	33.31	33.56	33.50
79	900	500	33.06	33.90	32.90
80	900	550	33.26	33.90	33.21
81	1000	550	33.11	32.70	33.79
82	1000	600	33.61	32.94	33.60
83	850	400	33.42	33.69	33.49
84	1000	150	33.82	33.03	32.84
85	1000	100	33.58	33.03	33.48
86	1000	500	33.03	32.64	33.49
87	1100	150	33.98	33.40	34.33
88	1100	300	33.97	32.73	34.11
89	1100	500	33.08	33.90	33.48
90	1200	500	33.60	33.74	33.60
91	1150	600	33.54	32.74	33.72

Table A-3 (continued)

Piez #	Coordinates (meters)		Pressure Heads (meters)		
	X	Y	02/03	04/14	06/30
92	1050	400	34.78	33.40	33.90
93	1200	300	33.05	33.37	32.80
94	300	200	33.79	33.41	33.67
95	300	0	33.21	32.75	34.57
96	200	150	33.61	33.42	33.53
97	200	200	33.36	33.90	34.28
98	200	550	34.36	33.29	34.12

Table A-4:   Geographic Coordinates.

| Piez. # | coordinates (meters) | | Elevation (centimeters) |
	X	Y	Z
1	150	200	173
2	100	150	183
3	50	150	180
4	50	50	176
5	50	250	173
6	150	250	234
7	200	450	217
8	50	350	193
9	150	500	190
10	100	500	187
11	50	550	202
12	100	650	231
13	100	700	203
14	200	600	219
15	200	650	214
16	150	350	181
17	0	350	189
18	300	400	129
19	350	350	219
20	40	250	167
21	60	350	184
22	650	350	153
23	650	500	170
24	700	450	202
25	600	450	219
26	550	500	214
27	450	500	205
28	450	700	234
29	400	600	183
30	350	600	219
31	550	750	251
32	500	850	226
33	650	600	233
34	600	650	238
35	600	800	288
36	700	650	240
37	700	700	254
38	700	750	252
39	750	750	187
40	750	850	204
41	750	700	234
42	800	750	120
43	800	650	243
44	900	700	208
45	950	700	204

Table A-4 (continued)

Piez #	Coordinates (meters)		Elevation (centimeters)
	X	Y	Z
46	1050	700	188
47	1150	700	170
48	1100	800	134
49	1200	800	195
50	1050	850	196
51	1000	800	214
52	900	800	216
53	800	800	218
54	800	500	221
55	300	150	136
56	300	150	164
57	350	50	234
58	400	150	185
59	450	150	145
60	450	200	166
61	450	100	125
62	500	50	120
63	550	0	134
64	550	150	139
65	600	50	215
66	650	150	153
67	750	150	114
68	750	200	172
69	750	250	124
70	800	250	129
71	800	200	86
72	850	200	127
73	850	100	147
74	900	100	113
75	900	150	103
76	800	500	127
77	950	300	187
78	950	400	106
79	900	500	86
80	900	550	77
81	1000	550	92
82	1000	600	220
83	850	400	98
84	1000	150	93
85	1000	100	55
86	1000	500	146
87	1100	150	79
88	1100	300	224
89	1100	500	222
90	1200	500	148

Table A-4 (continued)

Piez #	Coordinates (meters)		Elevation (centimeters)
91	1150	600	155
92	1050	400	185
93	1200	300	138
94	300	200	156
95	300	0	182
96	200	150	170
97	200	200	191
98	200	550	226

Kriging Results

RESULTATS

PEP	ERREUR MOY.	VAR. D'ERREUR	(Zm-Ze)/Ve	(Zm-Ze)/Ve (*)
.3	9.224991E-03	.6728318	1.215292	1.215292
.35	9.224993E-03	.672832	1.1901	1.1901
.4	9.224996E-03	.672832	1.166816	1.166816
.45	9.224996E-03	.672832	1.145194	1.145194
.5	9.224993E-03	.672832	1.125032	1.125032
.55	9.224998E-03	.6728319	1.106161	1.106161
.6	9.224996E-03	.6728318	1.08844	1.08844
.65	9.22499E-03	.672832	1.071749	1.071749
.7000001	9.224998E-03	.6728318	1.055985	1.055985
.75	9.224998E-03	.672832	1.041061	1.041061
.8	9.22499E-03	.672832	1.026899	1.026899

1-REAFFICHER   *   2-SUITE

(*) (Exclusion des cas Zm-Ze>2.5*Ec.Type)

1FIN   2   3   4   5   6   7   8   9   10

APPENDIX B

Computer Program Listing

```
1000 DEFINT I-N: KEY OFF: GOSUB 9800
1100 PRINT "---  Groundwater Modeling"
1200 PRINT "---  Finite Element Method"
1300 PRINT "---  Quadrangular elements"
1400 PRINT "---  By Boubacar BARRY": PRINT : PRINT
1500 DIM XJ(4), YJ(4), b(3), c(3), ks(4, 3), D(3)
1600 DIM x(500), y(500), IP(500), f(500), Fa(500), q(500)
1650 DIM U(500), V(500), W(500)
1700 DIM P(500, 11), KP(500, 11), NP(400, 4), T(400)
1750 DIM S(400), PP(400), R(400, 11): NZ = 11
1800 INPUT "Number of nodes .......... "; n
1900 INPUT "Number of elements ....... "; M
1950 INPUT "Maximum error.............."; E
2000 FOR i = 1 TO n
        GOSUB 6600
          NEXT i
     FOR j = 1 TO M
         GOSUB 7300
             NEXT j
2100 GOSUB 9800
     PRINT "Present input data (Y/N) ......... ? ";
2200 GOSUB 9500
     IF a$ = "N" THEN 2400
2300 FOR i = 1 TO n
        GOSUB 7900
     NEXT i
     FOR j = 1 TO M
         GOSUB 8600
     NEXT j
2400 FOR i = 1 TO 4
     FOR j = 1 TO 3
        K = i + j - 1
        IF K > 4 THEN K = K - 4
2500 ks(i, j) = K
     NEXT j, i
     GOSUB 9800
PRINT "Generation of pointer matrix"
2600 FOR i = 1 TO n
        KP(i, 1) = i
        KP(i, NZ) = 1
     NEXT i
2700 PRINT "   Element ...... ";
     FOR j = 1 TO M
PRINT j;
2800 FOR K = 1 TO 4
        KK = NP(j, K)
     FOR L = 1 TO 4
        LL = NP(j, L)
2900 IA = 0
     FOR II = 1 TO KP(KK, NZ)
        IF KP(KK, II) = LL THEN IA = 1
3000 NEXT II
        IF IA = 0 THEN KB = KP(KK, NZ) + 1
        KP(KK, NZ) = KB
        KP(KK, KB) = LL
```

```
3100 IF KB = NZ THEN 6500
3200 NEXT L, K, j
PRINT : PRINT
      EE = .00001

3210 PRINT "Generation of system matrices"
PRINT "    Element ...... ";
3220 FOR j = 1 TO M
PRINT j;
        FOR KW = 1 TO 4
            ZX = 0: ZY = 0
3230 FOR i = 1 TO 3
            K = NP(j, ks(KW, i))
            XJ(i) = x(K)
            YJ(i) = y(K)
3240 ZX = ZX + x(K)
            ZY = ZY + y(K)
     NEXT i
            ZX = ZX / 3
            ZY = ZY / 3
3245 FOR i = 1 TO 3
            XJ(i) = XJ(i) - ZX
            YJ(i) = YJ(i) - ZY
     NEXT i
3250 b(1) = YJ(2) - YJ(3)
      b(2) = YJ(3) - YJ(1)
      b(3) = YJ(1) - YJ(2)
3255 c(1) = XJ(3) - XJ(2)
      c(2) = XJ(1) - XJ(3)
      c(3) = XJ(2) - XJ(1)
3260 D(1) = XJ(2) * YJ(3) - XJ(3) * YJ(2)
      D(2) = XJ(3) * YJ(1) - XJ(1) * YJ(3)
3265 D(3) = XJ(1) * YJ(2) - XJ(2) * YJ(1)
3270 D = ABS(D(1) + D(2) + D(3))
      IF D < EE THEN 4040
3275 DD = T(j) / (4 * D)
      DE = S(j) / (4 * (1 - E) * D)
3280 XX = (XJ(1) * XJ(1) + XJ(2) * XJ(2)
            + XJ(3) * XJ(3)) / 12
3285 XY = (XJ(1) * YJ(1) + XJ(2) * YJ(2)
            + XJ(3) * YJ(3)) / 12
3290 YY = (YJ(1) * YJ(1) + YJ(2) * YJ(2)
            + YJ(3) * YJ(3)) / 12
3295 FOR K = 1 TO 3
      KK = NP(j, ks(KW, K))
      II = KP(KK, NZ)
    FOR LL = 1 TO II: L = 1
4000 KV = ks(KW, L)
      IF NP(j, KV) = KP(KK, LL) THEN 4015
4010 L = L + 1
        IF L < 4 THEN 4000 ELSE 4030
4015 P(KK, LL) = P(KK, LL) + DD * (b(K) * b(L) + c(K) * c(L))
4020 aa = XX * b(K) * b(L) + XY * (b(K) * c(L) + b(L) * c(K))
            + YY * c(K) * c(L) + D(K) * D(L)
```

```
4025 R(KK, LL) = R(KK, LL) + DE * aa
4030 NEXT LL, K
4035 FOR i = 1 TO 3
        K = NP(j, ks(KW, i))
        q(K) = q(K) + D * PP(j) / 12
     NEXT i
4040 NEXT KW, j
PRINT : PRINT : PRINT
        tn = 0: EE = EE * EE
PRINT "time ="; tn

4045 INPUT "Time after next step "; tt
        it = 1
        dt = tt - tn
           IF dt <= 0 THEN 5900
4050 b = 1 / dt
        tn = tt
PRINT "Solution of equations"
PRINT "   Iteration "; it
4055 FOR i = 1 TO n
        U(i) = 0
         IZ = KP(i, NZ)
           IF IP(i) > 0 THEN 4075
4060 U(i) = q(i)
     FOR j = 1 TO IZ
         L = KP(i, j)
4070 U(i) = U(i) - P(i, j) * f(L)
   NEXT j
4075 V(i) = U(i)
     NEXT i
        UU = 1
     FOR i = 1 TO n
        UU = UU + U(i) * U(i)
     NEXT i
4080 PRINT it;
     FOR i = 1 TO n
        W(i) = 0
           IZ = KP(i, NZ)
4085 FOR j = 1 TO IZ
        W(i) = W(i) + (P(i, j) + b * k(i, j)) * V(KP(i, j))
     NEXT j, i
4090 VW = 1
     FOR i = 1 TO n
        VW = VW + V(i) * W(i)
        NEXT i
4095 aa = UU / VW
     FOR i = 1 TO n
       IF IP(i) > 0 THEN 5100
5000 f(i) = f(i) + aa * V(i)
     U(i) = U(i) - aa * W(i)
5100 NEXT i
     WW = 0
     FOR i = 1 TO n
       WW = WW + U(i) * U(i)
     NEXT i
```

```
5200 BB = WW / UU
     FOR i = 1 TO n
         V(i) = U(i) + BB * V(i)
     NEXT i
         UU = WW
5300 it = it + 1
         IF it <= n AND UU > EE THEN 4080
5400 FOR i = 1 TO n
             Fa(i) = Fa(i) + (f(i) - Fa(i)) / (1 - E)
             f(i) = Fa(i)
         NEXT i


5500   GOSUB 9800: a$ = "####.##"
         FOR i = 1 TO n
5600   PRINT " - x = ";
       PRINT USING a$; x(i);
       PRINT "  - y = ";
5650   PRINT "  - x = ";
       PRINT USING a$; x(i);
       PRINT "  - y = ";
5700   PRINT USING a$; y(i);
       PRINT "  - f = ";
       PRINT USING a$; Fa(i)
5750   LPRINT USING a$; y(i)
       LPRINT "  - f = ";
       LPRINT USING a$; Fa(i)
5800       NEXT i
       PRINT "time = "; tn
       PRINT "Time = "; tn
       PRINT : GOTO 4045
5900   PRINT : END
5950   LPRINT : END
6500   GOSUB 9800
       PRINT "Pointer width (NZ) too small."
       PRINT : GOTO 5900
6600 GOSUB 9800: PRINT "Data of node "; i: PRINT : PRINT
6700 INPUT " x ................. "; x(i)
6800 INPUT " y ................. "; y(i)
6900 PRINT " Head given (Y/N) .. ? "; : GOSUB 9500
7000 IF a$ = "Y" THEN IP(i) = 1:  INPUT " F ................. "; f(i)
7100 IF a$ = "N" THEN IP(i) = -1: INPUT " Q ................. "; q(i)

7200 RETURN
7300 GOSUB 9800: PRINT "Data of element "; j: PRINT : PRINT
7400 INPUT "Node 1 ............. "; NP(j, 1)
7500 INPUT "Node 2 ............. "; NP(j, 2)
7600 INPUT "Node 3 ............. "; NP(j, 3)
7700 INPUT "Node 4 ............. "; NP(j, 4)
7800 INPUT "Transmissivity ..... "; T(j)
7805 INPUT "Storativity......... "; S(j)
7810 INPUT "Re(dis)charge....... "; PP(j): RETURN
```

```
7900 GOSUB 9800: PRINT "Node "; i: PRINT : PRINT
8000 PRINT " x ................. "; x(i)
8100 PRINT " y ................. "; y(i)
8200 IF IP(i) > 0 THEN PRINT " F ................. "; f(i)
8300 IF IP(i) < 0 THEN PRINT " Q ................. "; q(i)
8400 GOSUB 9400: IF a$ = "N" THEN GOSUB 6600: GOTO 7900
8500 RETURN
8600 GOSUB 9800: PRINT "Element "; j: PRINT : PRINT
8700 PRINT "Node 1 ............ "; NP(j, 1)
8800 PRINT "Node 2 ............ "; NP(j, 2)
8900 PRINT "Node 3 ............ "; NP(j, 3)
9000 PRINT "Node 4 ............ "; NP(j, 4)
9100 PRINT "Transmissivity ..... "; T(j)
9105 PRINT "Storativity.........."; S(j)
9110 PRINT "Re(dis)charge........"; PP(j)

9200 GOSUB 9400: IF a$ = "N" THEN GOSUB 7300: GOTO 8600
9300 RETURN
9400 PRINT : PRINT : PRINT "Correct (Y/N) ......? ";
9500 a$ = INPUT$(1): IF a$ = "Y" OR a$ = "y" THEN PRINT "Yes": a$ = "Y": RETURN
9600 IF a$ = "N" OR a$ = "n" THEN PRINT "No": a$ = "N": RETURN
9700 GOTO 9500
9800 CLS : LOCATE 1, 30, 1: COLOR 0, 7
9900  PRINT : COLOR 0, 7: PRINT : RETURN
     END
```
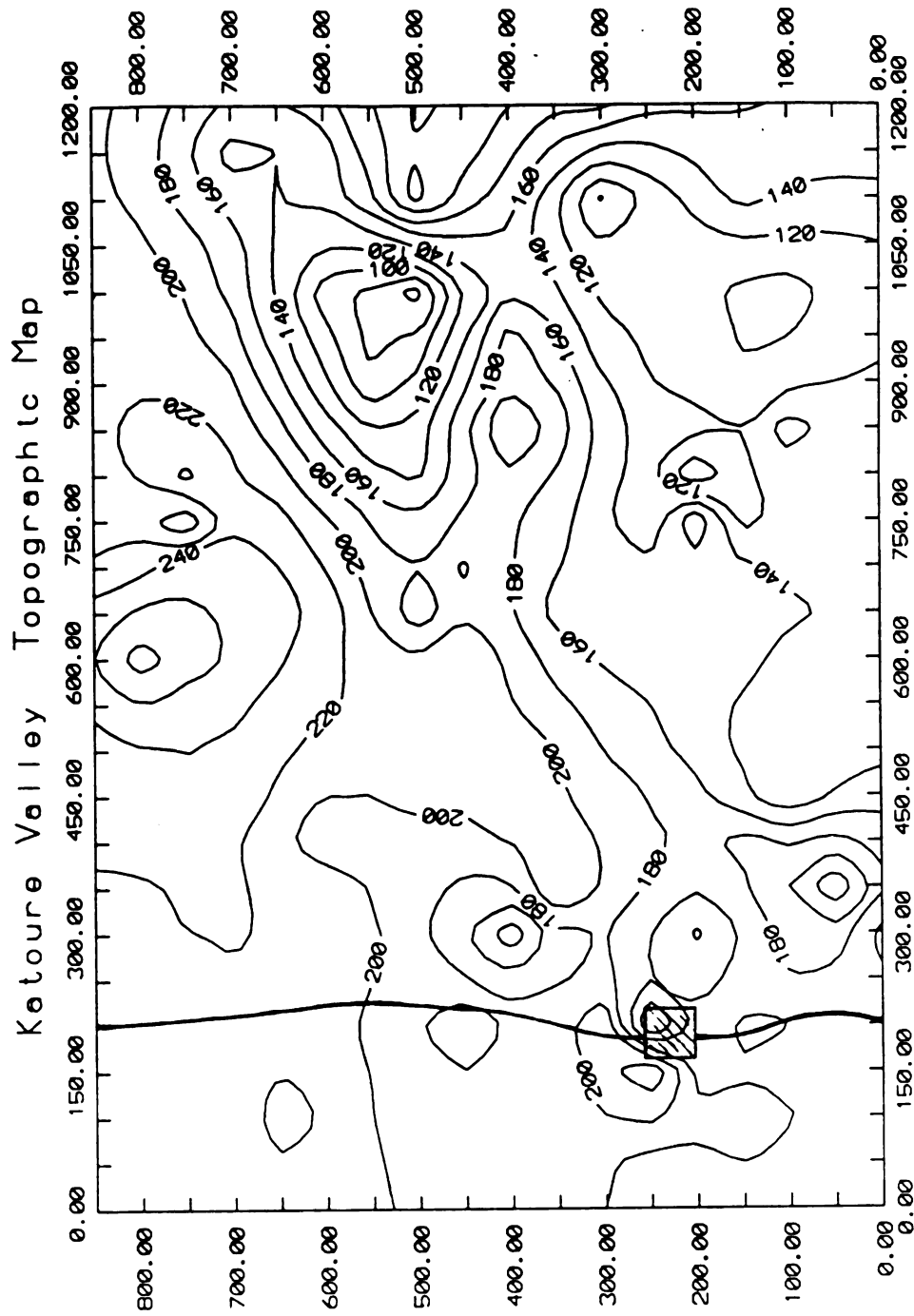
APPENDIX C

Simulation Results

Figure C-1. Topographic maps of Katoure Valley.
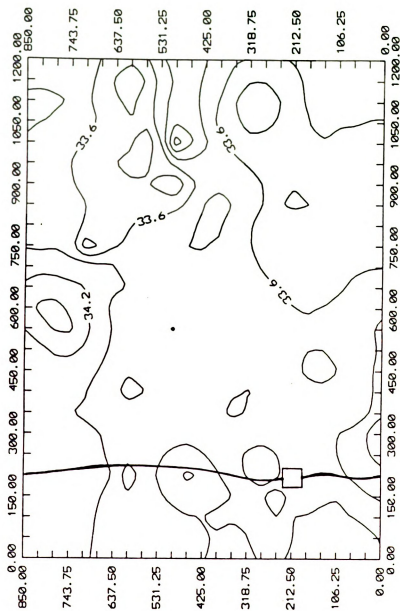
Figure C-2. Three-dimensional map of Katoure Valley.

Figure C-3. Predicted piezometric heads by the developed computer model for the Katoure Valley on February 03, 1987.
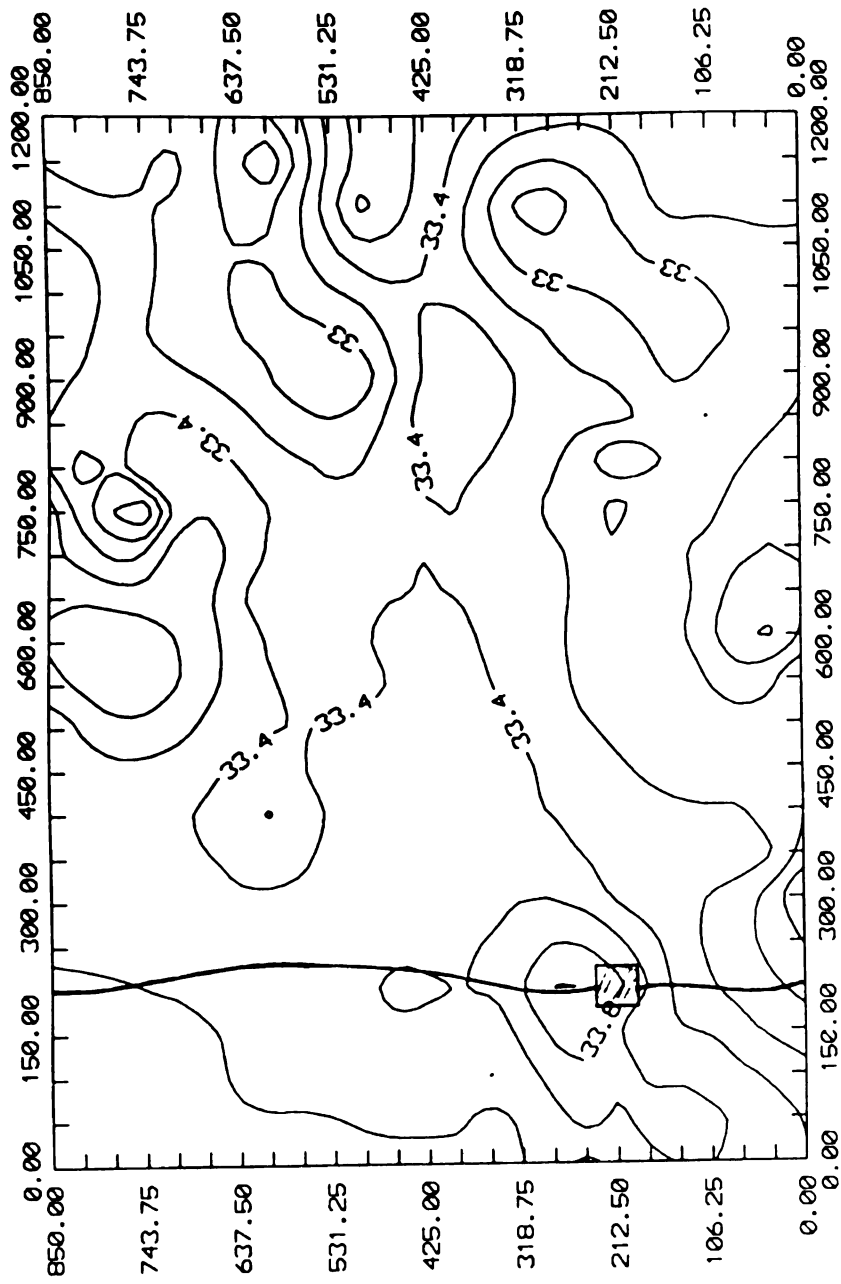
Figure C-4. Predicted piezometric heads by the developed computer model for the Katoure Valley on April 04, 1987.
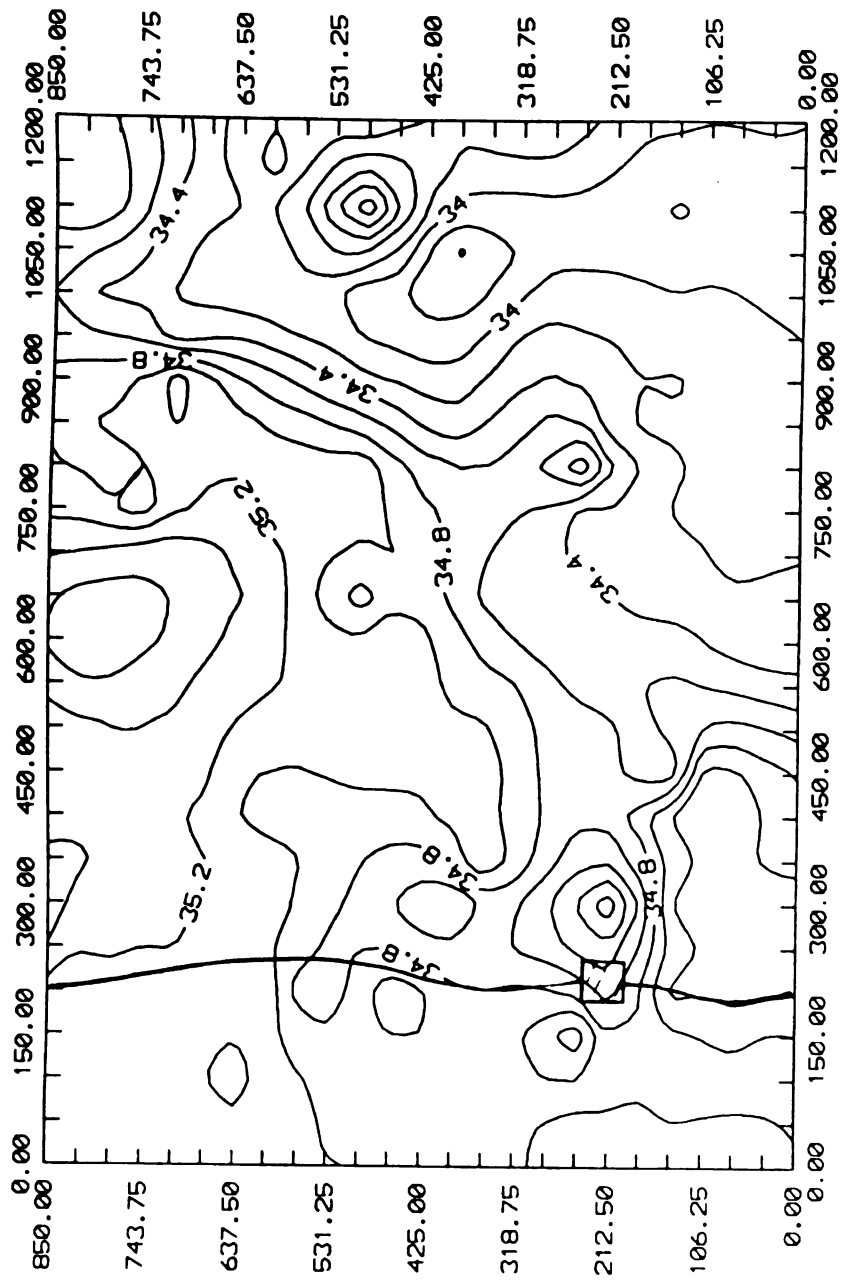
Figure C-5. Predicted piezometric heads by the developed computer
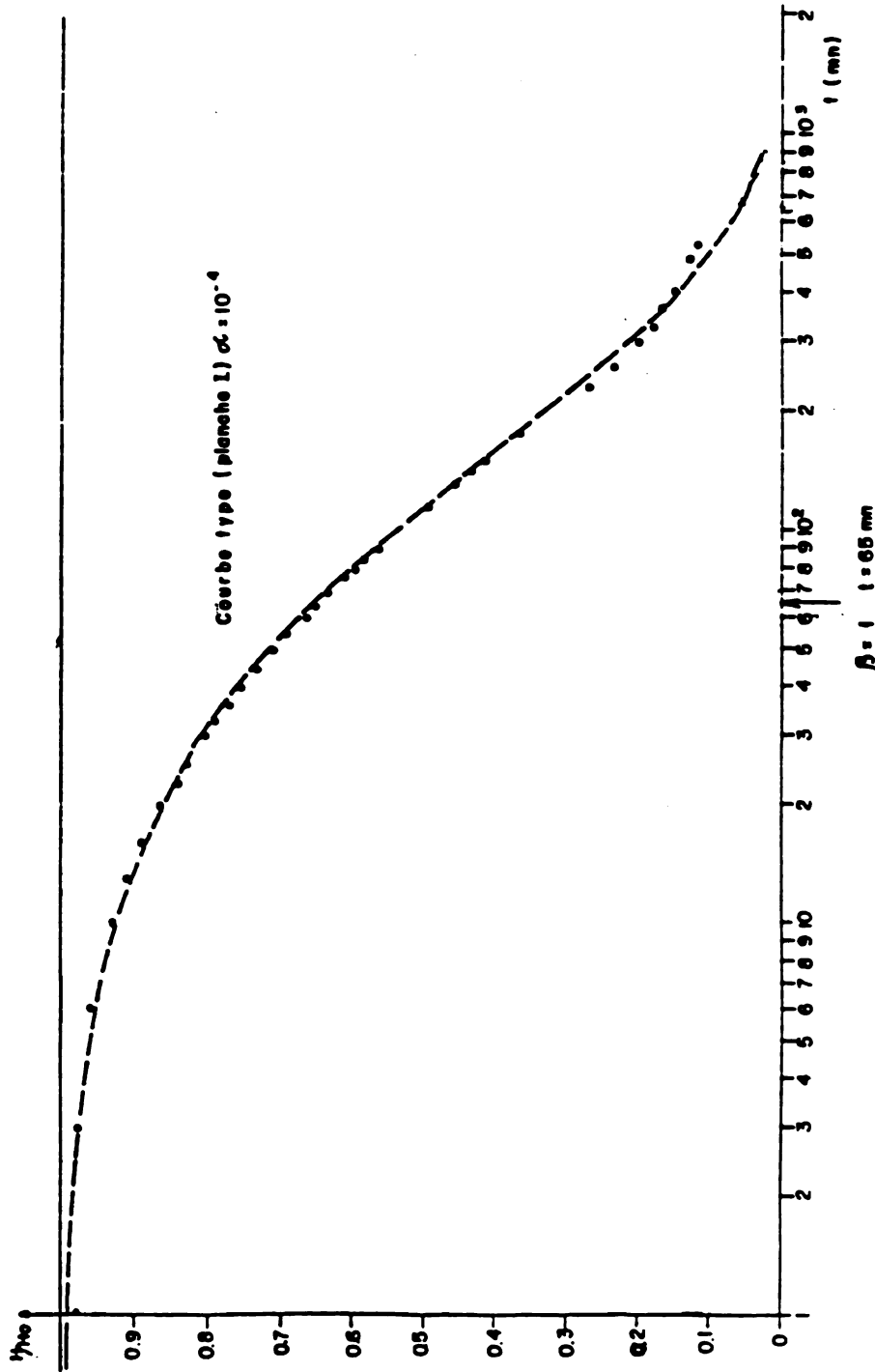model for the Katoure Valley on June 30, 1987.

Figure C-6. Characteristic curve for slug test.

REFERENCES

BCEOM-IRAT. 1970. Etude Economique et Technique du
Barrage du Kamoubeul. Ministere du Development rural.
Dakar, Senegal.

Bear J., and A. Verruijit. 1987. _Modeling Groundwater Flow
and Pollution_. Reidel Publishing Company, Dordrecht,
Holland.

Beye, G. 1973. Bilan de cinq annees d'Etudes du Dessalement
des Sols du Polder de Medina. Mimeo ISRA/CRADjibelor,
Senegal.

Bralts, V.F., D.M. Edwards and I-Pau Wu. 1987. Drip
irrigation design and evaluation based on the statistical
uniformity concept. In: _Advances in Irrigation._ Volume
4, D. Hillel (editor), Academic Press, New York. pp. 67-
117.

Bucks, D.A., F.S. Nakayama, and A.W. Warrick. 1982.
Principles, practices, and potentialities of trickle
irrigation. In: _Advances in Irrigation_. Volume 1.
Academic Press, New York. pp 219-298.

Club du Sahel. 1979. Strategy and Programs for Drought
Control. Organization for Economic Cooperation and
Development, Ottawa.

Cooper, H.H., J.D. Breddehoeft, and I.S. Papadopoulos. 1967.
Response of a finite diameter well to an instantaneous
charge of water. _Water Resources Res._ 3:263-269.

Dedrick, A.R. 1982. Level-basin irrigation. In: _Advances
in Irrigation._ Volume 1, D. Hillel (Editor) Academic
press, New York. pp 105-145.

Ediafric. 1982. Etudes Economiques du Senegal. La filiere
cerealiere. Ministere du Developement Rural, Dakar,
Senegal.

FAO. 1986. Consultation on Irrigation in Africa. Food and
Agricultural Organization of the United Nations, Irrigation
and Drainage Paper # 42, Rome, Italy.

FAO. 1984. Agriculture: Toward 2000. Food and Agricultural
Organization of the United Nations, Rome, Italy.

GeoStat. 1986. Universal kriging software. Office de
Recherche Scientifique et Technique d'outre Mer, Paris,
France.

GeoStat. 1971. Universal kriging. Office de Recherche Scientifique et Technique d'outre Mer, Paris, France.

Harza Engineering. 1981. Hydrology Report. Agriculture Division Section, Harza Engineering, Chicago, IL.

Heerman, D.F. and D.L. Swendensky. 1984. Simulation analysis of center pivot sprinkler uniformity. ASAE Paper No. 84-2582. ASAE, St. Joseph, MI.

Hvorslev, M.J. 1951. Time lag and soil permeability in groundwater observations. U.S. Army Corps of Engineers Waterways Exp. Sta. Bull. 36, Vicksburg, Miss.

Kemper, W.D., W.H. Heinemann, D.C. Kincaid, R.V. Le Prion, and B. Dieng. 1986. Etude Hydrogeologique de la Casamance. Cahier de l'ORSTOM, Dakar, Senegal.

Kinzelbach W. 1986. Groundwater Modelling: An Introduction with Sample Programs in Basic. Elsevier, Amsterdam, Holland.

Lyle, W. and J.P. Bordovsky. 1983. LEPA irrigation system evaluation. Transactions of the American Society of Agricultural Engineers. 26: 776-81.

Marius, C. and M. Cheval. 1980. Note sur les Sols de la Vallee de Guidel. ORSTOM, Dakar, Senegal.

Papadopoulos, I.S., J.D. Bredehoeft, and H.H. Cooper. 1973. On analysis of the slug test data. Water Resources Research., 9:1087-1089.

Plusquellec, H. 1985. The silent minority. World Bank 4(1):13-15.

Reddy, J.N. 1984. An Introduction to the Finite Element Method. McGraw-Hill Book Company, New York, NY.

Schillinger. 1978. Le Potential Agronomique de la Region, Volume 2. Master Plan for Rural Development of the Casamance Region, Somivac. Ziguinchor, Senegal.

Segerlind, L.J. 1984. Applied Finite Element Analysis. (Second Edition). Wiley and Sons, New York, NY.

Zienkiewcz, O.C. 1977. The Finite Element Method in Structural and Continuum Mechanics. McGraw-Hill, New York.